Accepted Manuscript

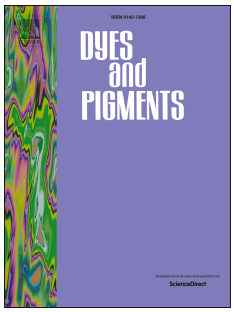

2,6-Anthracenyl(anthraquinonyl)-Substituted Difluoroboron Dipyrromethenes: Synthesis, Spectroscopy, Electrochemistry and Quantum Chemical Calculations

Liang Xu, Yongjun Li, Runsheng Jiang, Zhihong Qin, Yuliang Li

PII: S0143-7208(14)00112-0

DOI: 10.1016/j.dyepig.2014.03.032

Reference: DYPI 4320

To appear in: *Dyes and Pigments*

Received Date: 7 December 2013

Revised Date: 17 March 2014

Accepted Date: 25 March 2014

Please cite this article as: Xu L, Li Y, Jiang R, Qin Z, Li Y, 2,6-Anthracenyl(anthraquinonyl)-Substituted Difluoroboron Dipyrromethenes: Synthesis, Spectroscopy, Electrochemistry and Quantum Chemical Calculations, *Dyes and Pigments* (2014), doi: 10.1016/j.dyepig.2014.03.032.

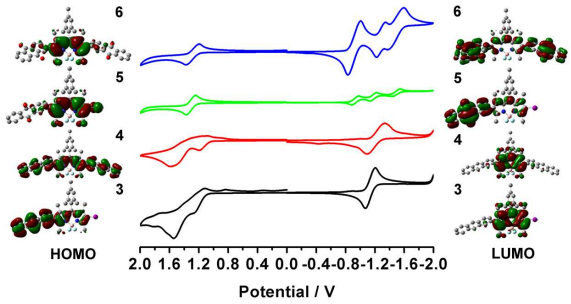

Suzuki coupling reactions of 2,6-diiodo-8-Mesityl-1,3,5,7-tetramethyl-4,4-difluoro-4-bora-3a,4a-diaza-s-indacene and 2-anthracen(anthraquinon)-2-yl-4,4,5,5-tetramethyl-[1,3,2] dioxaborolane gave several novel core-expanded Bodipy chromophores along the long axis. Their properties were investigated by spectroscopy, electrochemistry and quantum chemical calculations, and an intramolecular charge-transfer process was proved.

2,6-Anthracenyl(anthraquinonyl)-Substituted Difluoroboron Dipyrromethenes: Synthesis, Spectroscopy, Electrochemistry and Quantum Chemical Calculations

Liang Xu[a,b], Yongjun Li[a]*, Runsheng Jiang[a,b], Zhihong Qin[a,b], Yuliang Li[a]*

[a]Beijing National Laboratory for Molecular Sciences (BNLMS), CAS Key Laboratory of Organic Solids, Institute of Chemistry, Chinese Academy of Sciences, Beijing 100190, P.R.

[b]University of Chinese Academy of Sciences, Beijing 100049, P.R. China

ABSTRACT

A series of anthracenyl(anthraquinonyl)-substituted difluoroboron dipyrromethene dyes were synthesized through a Suzuki cross-coupling reaction. The crystal structure combined with geometric optimization reveals a moderate dihedral angle between the anthracenyl(anthraquinonyl) plane and the connected pyrrolyl plane. Photophysical characterization shows that the introduction of anthracenyl(anthraquinonyl) moiety to the BODIPY core effectively tunes the emission properties of BODIPY while retaining the separate absorption properties of BODIPY and anthracene(anthraquinone). High fluorescent quantum yields of up to 0.70 and a large Stokes shift (ca. 1707 cm^{-1}) were noted. Electrochemical characterization suggests that the anthracenyl(anthraquinonyl) linkage and BODIPY unit lead to rich and tunable potentials. TD-DFT calculation proved a moderate intramolecular charge-transfer process between the BODIPY core and anthracenyl(anthraquinonyl) moiety.

Keywords:

Anthracene; Anthraquinone; BODIPY; Donor-acceptor; Gaussian calculation; Intramolecular charge-transfer

1. Introduction

Recently, BODIPY (4,4-difluoro-4-bora-3a,4a-diaza-*s*-indacene) has drawn widespread attention in the chemical and biological society due to the diverse applications as biological labels,[1, 2] chemosensors,[3-8] fluorescent switches,[9, 10] laser dyes,[11] drug delivery,[12] electroluminescent films,[13] and as dye-sensitized solar cells.[14, 15] Similar to *s*-indacene dyes, a proximate coplanar geometry for the central six-membered ring and the adjacent five-membered ring is found in BODIPY dyes, which facilitate in delocalizing the π-electron over the entire BODIPY core. Different substitution reaction patterns, as well as different reactive sites on the core enrich the modifications to BODIPY. To BODIPY dye of which alkylation and arylation are the most common. The meso site favors an orthogonal conformation for aryl groups because of the steric hindrance effect.[16] The restriction of meso-aryl rotation by introducing alkyl groups to the 1,7-positions is a common route to enhance the fluorescence quantum yield because it reduces the energy loss through non-irradiative transition in excited states.[17] Consistent with this, alkyl groups are also often introduced to the meso-aryl ring. For 2- and 6-position, electrophilic substitution is also likely to occur because these two sites have the least positive charge in the resonance structures.[18] For the boron, Grignard reagents or aryl lithium reagents are needed for alkylation or arylation. Generally, the B–F bonds are inert to Sonogashira, Heck, Suzuki and other cross-coupling reactions.

BODIPY is intrinsically electron rich, which is usually served as an electron-donor. Sometimes, it also plays a part in the scope of electron-acceptor.[19-21] In order to realize the switching between its dual roles, strong electron-acceptor and donor are needed to increase the permanent dipole moment strength of monosubstituted BODIPY.[22] Holding high hole mobilities,

anthracene is recognized as a candidate for p-type semiconductor for organic field-effect transistors (OFETs).[23] The extension of the π-conjugation of anthracene unit may provide efficient charge transportation system.[24] Besides electron-donating nature, anthracene is also a fine chromophore with high fluorescence. These properties of anthracene remind us of another chromophore-anthraquinone, which has the opposite features. 9, 12-anthraquinone (AQ) is highly electrophilic and easily incorporated to π-conjugated systems.[25, 26] Besides, AQ shows a high intersystem crossing efficiency (Φisc), thus, it significantly reduces the fluorescent quantum yields.[27, 28] The BODIPY derivatives having a direct connection between the BODIPY core and 9-anthracenyl moiety is apt to adopt a twisted conformation, thus the BODIPY core and anthracene (or anthraquinone) is partly electronically independent and the conjugation is altered to some extent.[20]

8-Phenyl-4,4-difluoro-1,3,5,7-tetramethyl-4-bora-3a,4a-diaza-*s*-indacene is highly fluorescent.[29] The attachment of methyl groups to the 1,7-positions of BODIPY and to ortho, para-positions of the 8-aryl ring restrain the aryl ring from revolving around the single bond, contributing to a large fluorescence quantum yield.[4] Thus, the fluorescent quantum yield of 8-mesityl-1,3,5,7-tetramethyl-4,4-difluoro-4-bora-3a,4a-diaza-*s*-indacene is reported to be 0.97.[30] The introduction of methyl groups at 1,3,5,7-positions of BODIPY also have an impact on the orientation of the substituting groups at 2,6-positions, leading to a nonplanar conformation. From the reported 2,6-diiodosubstituted BODIPY dye,[31-37] monosubstituted products (**3** and **5)** and disubstituted products (**4** and **6**) are achieved under one-pot condition. (Scheme 1) The aim of extending the conjugation along the long axis of BODIPY core is to make it still feasible for

charge transfer between BODIPY core and anthracenyl (or anthraquinonyl) part in spite of nonplanar geometry.[38]

2. Experimental

2.1 Reagents and instruments

Most reagents were purchased from Alfa Aesar or Aldrich and used as supplied unless otherwise noted. All the solvents used in photophysical measurements and electrochemical measurements were of HPLC grade quality. All other solvents were obtained commercially and purified using standard procedures. Silica gel with 200-300 mesh were used in column chromatography, and precoated silica gel plates were utilized in thin-layer chromatography (TLC) and monitored by UV light. SHIMADZU GCMS-QP2010 puls spectrometer was employed in EI mass spectrometric measurements. Bruker Biflex III mass spectrometer was engaged in Matrix-assisted laser desorption/ionization reflectron time-of-flight (MALDI-TOF) mass spectrometry. Nuclear magnetic resonance (NMR) spectra were measured on Bruker Avance DPS-400 spectrometer at room temperature (298 K), and chemical shifts were referenced to the residual solvent peaks. Elemental analyses were recorded on a Carlo-Erba-1106 instrument. UV-Vis spectra were performed on a Hitachi U-3010 spectrometer, and Fluorescence emission spectra were monitored using a Hitachi F-4500, which is corrected for the wavelength dependence of the throughput of the emission monochromator and of the sensitivity of the detector.

Cyclic voltammetry measurements were monitored on a CHI660D electrochemical workstation (CH Instruments, Austin, TX). A dry weighing bottle was served as the container. The working electrode glassy carbon (3.0 mm in diameter) was polished on a felt pad with 0.05μm alumina (Buehler, Ltd., Lake Bluff, IL), sonicated in deionized water for 2 min, and then dried before

usage. The counter electrode platinum wire was rubbed with an abrasive paper, washed with deionized water and acetone, and dried. The reference electrode saturated calomel electrode (SCE) was washed with deionized water and also dried. The CV experiment was conducted under N_2 atmosphere with *n*-Bu_4NPF_6 as the supporting electrolyte. The scan rate was 50 mV/s.

2.2 Synthesis procedures and characterization data for new compounds

Synthesis of compounds **3** and **4**

To a stirred, degassed solution of compound **2** (310 mg, 0.5 mmol) and 2-anthracen-2-yl-4,4,5,5-tetramethyl-[1,3,2]dioxaborolane (304 mg, 1.0 mmol) in DMF (35 mL), K_2CO_3 (414 mg, 3.0 mmol) dissolved in a minimum amount of water was added. The mixture was stirred at room temperature under argon for 10 minutes. Then Pd $(PPh_3)_4$ (58 mg, 0.05 mmol) was added. The mixture was then heated at 80°C for 12 h under argon. The reaction mixture was concentrated in vacuo, and the resulting solid was dissolved in CH_2Cl_2 (50 mL), washed with H_2O (1×20 mL) and dried over anhydrous Na_2SO_4. Concentrated in vacuo and purified by column chromatography (CH_2Cl_2/petroleum ether=1/1), affording compounds **3** (127 mg, yield 38%) and **4** (180 mg, yield 50%).

For compound **3**, m.p. 199-200°C. IR (KBr, cm^{-1}): 2922.58, 1534.75, 1456.46, 1396.11, 1351.41, 1311.27, 1212.57, 1179.72, 1115.27, 1086.89, 1003.29. ^{1}H NMR (400 MHz, $CDCl_3$) δ 8.44 (s, 1 H), 8.40 (s, 1 H), 8.03-8.01 (m, 3 H), 7.78 (s, 1 H), 7.48-7.46 (m, 2 H), 7.29 (s, 1 H), 6.98 (s, 2 H), 2.68 (s, 3 H), 2.62 (s, 3 H), 2.34 (s, 3 H), 2.16 (s, 6 H), 1.44 (s, 3 H), 1.40 (s, 3 H). ^{13}C NMR (100 MHz, $CDCl_3$) δ 156.40, 154.66, 142.79, 142.07, 140.39, 139.16, 135.71, 135.03, 134.97, 132.11, 132.03, 131.55, 131.31, 130.73, 130.36, 129.48, 129.38, 129.26, 128.36, 128.33, 128.27, 127.93, 126.38, 126.26, 125.76, 125.68, 21.38, 19.81, 16.04, 15.74, 13.91, 12.10. MS (MALDI-TOF) m/z

668.3 (M+). Anal. Calcd for $C_{36}H_{32}N_2BF_2I$, C, 64.69; H, 4.83; N, 4.19; Found C, 64.74; H, 4.82; N, 4.15.

For compound **4**, m.p. 212-213°C. IR (KBr, cm^{-1}): 2922.15, 1534.26, 1452.41, 1393.75, 1314.53, 1215.50, 1179.41, 1106.39, 1081.43, 1010.58, 904.79. ^{1}H NMR (400 MHz, $CDCl_3$) δ 8.45 (s, 2 H), 8.42 (s, 2 H), 8.05-8.01 (m, 6 H), 7.83 (s, 2 H), 7.49-7.46 (m, 4 H), 7.34 (d, *J* = 8.0 Hz, 2 H), 6.99 (s, 2 H,), 2.67 (s, 6 H), 2.33 (s, 3 H), 2.27 (s, 6 H), 1.45 (s, 6 H). ^{13}C NMR (100 MHz, $CDCl_3$) δ 154.30, 142.36, 138.89, 138.77, 135.05, 133.41, 132.05, 131.93, 131.65, 131.62, 130.82, 130.68, 129.31, 129.19, 128.32, 128.26, 128.24, 128.21, 126.31, 126.21, 125.68, 125.58, 21.38, 19.96, 13.78, 12.00. MS (MALDI-TOF) m/z 718.5 (M+). Anal. Calcd for $C_{50}H_{41}N_2BF_2$, C, 83.56; H, 5.75; N, 3.90; Found C, 83.60; H, 5.74; N, 3.88.

Synthesis of compounds **5** and **6**

The procedure was the same with above except that 2-anthraquinon-2-yl-4,4,5,5-tetramethyl-[1,3,2]dioxaborolane (334 mg, 1.0 mmol) was added instead of 2-anthracen-2-yl-4,4,5,5-tetramethyl-[1,3,2]dioxaborolane. This reaction gave compounds **5** (122 mg, yield 35%) and **6** (175 mg, yield 45%).

For compound **5**, m.p. 201-202°C. IR (KBr, cm^{-1}): 2964.77, 2922.35, 1675.17, 1594.68, 1533.38, 1460.25, 1394.98, 1349.22, 1312.57, 1292.45, 1263.20, 1228.57, 1180.67, 1116.75, 1080.62, 1006.09. ^{1}H NMR (400 MHz, $CDCl_3$) δ 8.36-8.30 (m, 3 H), 8.12 (s, 1 H), 7.82-7.80 (m, 2 H), 7.63-7.60 (m, 1 H), 6.99 (s, 2 H), 2.69 (s, 3 H), 2.58 (s, 3 H), 2.35 (s, 3 H), 2.14 (s, 6 H), 1.45 (s, 3 H), 1.37 (s, 3 H). ^{13}C NMR (100 MHz, $CDCl_3$) δ 183.19, 182.94, 156.41, 154.36, 144.23, 142.76, 140.23, 139.79, 139.38, 135.70, 134.92, 134.37, 134.27, 133.75, 133.68, 133.66, 132.19, 132.00, 131.18, 131.06, 130.58, 129.48, 128.79, 127.65, 127.42, 127.38, 21.37, 19.77, 16.16, 15.89, 13.70,

12.00. MS (MALDI-TOF) m/z 698.4 (M+), Anal. Calcd for $C_{36}H_{30}N_2O_2BF_2I$, C, 61.92; H, 4.33; N, 4.01; Found C, 61.95; H, 4.30; N, 3.99.

For compound **6**, m.p. 254-255°C. IR (KBr, cm^{-1}): 2922.83, 1677.08, 1594.55, 1531.61, 1472.26, 1435.55, 1391.94, 1317.13, 1232.19, 1183.27, 1115.26, 1095.81, 1011.63, 931.22. ^{1}H NMR (400 MHz, $CDCl_3$) δ 8.37-8.31 (m, 6 H), 8.15 (s, 2 H), 7.83-7.80 (m, 4 H), 7.66-7.64 (m, 2 H), 7.00 (s, 2 H), 2.63 (s, 6 H,), 2.34 (s, 3 H), 2.22 (s, 6 H), 1.42 (s, 6 H). ^{13}C NMR (100 MHz, $CDCl_3$) δ 183.21, 182.96, 154.14, 143.62, 140.25, 139.29, 135.73, 134.77, 134.38, 134.28, 133.64, 133.57, 133.56, 132.05, 131.82, 131.06, 130.99, 129.49, 128.77, 127.63, 127.39, 127.35, 21.37, 19.89, 13.70, 12.01. MS (MALDI-TOF) m/z 778.5 (M+). Anal. Calcd for $C_{50}H_{37}N_2O_4BF_2$, C, 77.13; H, 4.79; N, 3.60; Found C, 77.15; H, 4.80; N, 3.59.

For compound **7**, m.p. 246-247°C. IR (KBr, cm^{-1}): 2921.25, 1675.52, 1593.83, 1539.41, 1466.16, 1437.75, 1398.63, 1312.22, 1293.50, 1264.70, 1229.68, 1189.61, 1116.68, 1076.33, 1008.14, 985.23, 931.79. ^{1}H NMR (400 MHz, $CDCl_3$) δ 8.34-8.31 (m, 3H), 8.12 (s, 1 H), 7.82-7.79 (m, 2 H), 7.63-7.61 (m, 1 H), 6.97 (s, 2 H), 6.05 (s, 1 H), 2.61 (s, 3 H), 2.58 (s, 3 H), 2.33 (s, 3 H), 2.15 (s, 6 H), 1.42 (s, 3 H), 1.37 (s, 3 H). ^{13}C NMR (100 MHz, $CDCl_3$) δ 183.30, 183.03, 157.45, 152.00, 144.04, 142.65, 140.83, 139.03, 137.80, 135.79, 134.97, 134.32, 134.22, 133.78, 133.71, 133.59, 131.93, 131.81, 131.19, 130.90, 130.11, 129.32, 128.82, 127.56, 127.39, 127.36, 121.98, 21.35, 19.76, 14.95, 13.76, 13.49, 11.77. MS (MALDI-TOF) m/z 572.3 (M+). Anal. Calcd for $C_{36}H_{31}N_2O_2BF_2$, C, 75.53; H, 5.46; N, 4.89; Found C, 75.50; H, 5.48; N, 4.91.

3. Results and discussion

3.1. Synthesis of BODIPY dyes **3-6**

As shown in scheme 1, 8-mesityl-1,3,5,7-tetramethyl-4,4-difluoro-4-bora-3a,4a-diaza-*s*-indacene **1** and the 2,6-diiodosubstituted one **2** are prepared according to the literatures.[30, 31] Suzuki coupling reactions of compound **2** with either 2-anthracen-2-yl-4,4,5,5-tetramethyl-[1,3,2]dioxaborolane[24] or 2-anthraquinon-2-yl-4,4,5,5-tetramethyl-[1,3,2]dioxaborolane[39] give the desired anthracenyl-substituted products (**3** and **4**) and anthraquinonyl-substituted products (**5** and **6**). In the second case, very small amounts of compound **7** is obtained as a byproduct (<5%).

3.2. Crystal structures

Single crystal structure for compound **2** has been reported,[31] but that for compound **1** has not been reported yet. Although the single crystals for compounds **3-6** have not been obtained, the single crystals for compound **1** and **7** have been acquired by slow evaporation of dichloromethane solutions over two months. Compared to compound **5**, compound **7** lacks an iodine atom, so it can be used as a reference for compound **5**. As shown in figure 1 and table S2, the crystal system for compound **1** is orthorhombic, while that for compound **7** is monoclinic. The orientation of the 2,4,6-trimethylphenyl moiety is rotated out of the dipyrrolyl plane with a dihedral angle of 84.38° for compound **1** and 89.90° for compound **7**. For compound **1**, The average B－N and B－F bond lengths are 1.544 and 1.392 Å, respectively, and the average N-B-N, F-B-N and F-B-F angles are 107.22, 110.10, 109.18°, respectively. The C4－N1 and C10－N2 bond lengths are 1.348 and 1.355 Å, while C1－N1 and C7－N2 bond lengths are 1.396 and 1.395 Å.[40, 41] For compound **7**, The average B－N and B－F bond lengths are 1.546 and 1.392 Å, respectively, and the average N-B-N, F-B-N and F-B-F angles are 106.29, 110.50, 108.54°, respectively. The C16－N1 and C26－N2 bond lengths are 1.334 Å and 1.351 Å, while C20－N1 and C22－N2 bond lengths are

1.385 and 1.411 Å. The dihedral angle between anthraquinonyl moiety and the connected pyrrolyl plane is 48.48°. Due to the electron-withdrawing effect of anthraquinonyl group, the length of the C16－C17 bond (1.419 Å) in compound **7** is significantly longer than that of the C3－C4 bond (1.404 Å) in compound **1**. While the length of the C25－C26 bond (1.405 Å) in compound **7** is similar to that of the C9－C10 bond (1.402 Å) in compound **1**.[22]

The packing diagrams for compound **1** and **7** are also shown in figure 1. For compound **1**, there are four molecules in one crystal cell. Intermolecular hydrogen bondings between fluorine atoms and hydrogen atoms are the most important forces. There are three kinds of F－H hydrogen bondings. Along a axis, F－H hydrogen bonds are formed between the fluorine atom of difluoroboron moiety and the hydrogen atom of 4-methyl group of meso-aryl ring. Along b axis, F－H hydrogen bonds are formed between the fluorine atom of difluoroboron moiety and the hydrogen atom of 1(7)-methyl group of BODIPY core. Along c axis, F－H hydrogen bonds are formed between the fluorine atom of difluoroboron moiety and the hydrogen atom of 3(5)-CH group of meso-aryl ring. For compound **7**, there are also four molecules in one crystal cell. Along a axis, two intermolecular O－H hydrogen bonds are formed between the oxygen atoms of anthraquinonyl moiety and the hydrogen atoms of C－H group of anthraquinonyl group. Also two intermolecular N－H hydrogen bonds are formed between the nitrogen atoms of dipyrrolyl moiety and the hydrogen atoms of C－H group of anthraquinonyl group. Along b axis, F－H hydrogen bonds are formed between the fluorine atom of difluoroboron moiety and the hydrogen atom of C－H group of anthraquinonyl group. Also C－H$\cdots\pi$ interaction is observed between 2(6)-methyl group of meso-aryl ring and the carbon atom of anthraquinonyl unit. Along c axis, strong π-π stacking is observed between the anthraquinonyl group of one molecule and that of the other.

Therefore, the introduction of anthraquinonyl group at 2(6)-position not only alters the bond lengths and angles, but also affects the packing modes, which is also probably attributed to its electron-withdrawing nature.[42]

3.3. Geometric optimization

The optimization for geometric structures of compounds **1** and **3-6** is carried out by Gaussian 03 program at the B3LYP/6-31tG* level.[43] For compound **1**, the calculated bond lengths and angles are in good agreement with the crystallographic data except for some small deviations (Table S3), which suggests that this calculation method is suitable for our BODIPY system. Hence, it is feasible to investigate the structural information of compounds **3-6** under this optimization. As shown in figure 2, for compounds **3-6**, the dihedral angles between 8-mesityl plane and the dipyrrolyl plane are 88.85, 87.46, 88.28 and 89.84°, respectively. These proximately perpendicular geometries assist in alleviating the electronic-coupling effect.[44] The dihedral angle between anthracenyl plane and the connected pyrrolyl plane in compound **3** is 56.14°, which is 54.87° in compound **4**. The dihedral angle between anthraquinonyl plane and the connected pyrrolyl plane is 51.43° for compound **5** and 52.19° for compound **6**. These results confirm the twisted geometry for dipyrrolyl moiety and anthracenyl (or anthraquinonyl) moiety.

3.4. Photophysical properties

Images demonstrating the color and fluorescence emission of the compounds **3-6** are shown in Figure S4. Compounds **3**, **5** and **6** all display a magenta color, while compound **4** exhibits a red color. A light yellow color with strong fluorescent emission is observed in compound **4**, while a dark orange color with very weak fluorescence emission is monitored in compound **3**. The fluorescence emission for compound **5** and **6** are hardly discerned.

As shown in figure 3 and table 1, in comparison to compound **1** (λ_{max}=501 nm),[30] the UV-Vis spectra of compounds **3**, **4**, **5** and **6** display a combination of a red-shifted BODIPY unit (λ_{max} around 532 nm) and an anthracenyl (λ_{max}=253 nm) or an anthraquinonyl unit (200-300 nm)[45]. Compared to compound **2**, the UV-Vis spectra of compounds **3** and **4** show only small red shifts (2 and 6 nm) but the fluorescence spectra show relatively big red shifts (23 and 44 nm). These phenomena suggest that in the excited state there is a planarization of the molecules allowing a larger electronic interaction between the BODIPY core and the anthracenyl part. Although incorporating two high fluorescent anthracenyl moieties, the fluorescent quantum yield of compound **4** (0.70) is conversely smaller than that of compound **1** (0.97).[30] The reason for this is probably due to the intramolecular charge-transfer (ICT) between two fluorescent moieties.[46] Maybe this process and the heavy-atom effect combine to reduce the fluorescent quantum yield of compound **3** (0.06). To confirm the ICT formation, the absorption and fluorescence spectra of compound **4** in different solvents are also investigated (Figure S5-1 in the Supporting Information). With the polarity increasing in the order of ethyl ether, dichloromethane, THF, acetonitrile and DMF, the absorption spectra only show very small redshifts, but the fluorescence spectra show obvious redshifts. Besides, the fluorescent quantum yields of compounds **4** and **1** are also determined in these solvents. For compound **4**, the fluorescent quantum yields in ethyl ether, dichloromethane, THF, acetonitrile and DMF are 0.93, 0.70, 0.61, 0.21 and 0.18, respectively. For compound **1**, the fluorescent quantum yields in ethyl ether, dichloromethane, THF, acetonitrile and DMF are 0.99, 0.97, 0.88, 0.76 and 0.72, respectively. Compound **5** and **6** have the smallest fluorescent quantum yield (0.003). These dyes all exhibit considerable molar extinction coefficients (more than 6×10^5 $M^{-1}\cdot cm^{-1}$). Specifically, the extinction coefficients for compound **3**,

4, **5** and **6** are 85893 $M^{-1}\cdot cm^{-1}$ (λ_{max}=532 nm), 60268 $M^{-1}\cdot cm^{-1}$ (λ_{max}=536 nm), 70670 $M^{-1}\cdot cm^{-1}$ (λ_{max}=532 nm) and 93199 $M^{-1}\cdot cm^{-1}$ (λ_{max}=532 nm), respectively. The Stokes shift for compounds **3**, **4**, **5** and **6** are 1222, 1707, 615 and 779 cm^{-1}, respectively.

3.5. Electrochemical properties

The photophysical properties of compound **2** are reported, but its electrochemical properties are not reported yet. In our experiments, the redox potentials for compounds **2-6** are obtained by cyclic voltammetry (figure 4) and summarized in table 1. Compound **1** is reported to have one reversible oxidation potential (1.14 V vs. SCE) and one reversible reduction potential (-1.19 V vs. SCE).[30] In comparison to compound **1**, the reversible oxidation potential of compound **2** (1.49 V vs. SCE) is positively shifted by 0.35 V, and the reversible reduction potential (-0.91 V vs. SCE) is positively shifted by 0.28 V. Hence, the substitution of hydrogen by iodine atom renders the oxidation harder. Meanwhile, it seems a feasible route to improve the photostability of BODIPY derivatives by attaching iodo group to 2,6-positions of the BODIPY core.[52] For compound **3**, two irreversible oxidation potential (1.26, 1.54 V vs. SCE) and one reversible reduction potential (-1.14 V vs. SCE) are monitored. The first oxidation potential is mostly contributed by anthracenyl moiety, while the second oxidation potential is mostly contributed by the BODIPY core. Compared to compound **2**, the reduction potential for the BODIPY core of compound **3** negatively migrated by 0.23 V (vs. SCE), indicating that the substitution of one iodo group by anthracenyl unit renders the oxidation easier. For compound **4**, two irreversible oxidation potentials (1.20, 1.58V vs. SCE) and one reversible reduction potential (-1.21 V vs. SCE) are discerned. In comparison to compound **3**, the first oxidation potential mainly for anthracenyl moiety negatively shifted by 0.06 V (vs. SCE), and the reduction potential for BODIPY core

negatively shifted by 0.07 V (vs. SCE), which suggest an easier oxidation requirement. Compared to compound **1**, the reduction potential for the BODIPY core of compound **4** negatively shifted by 0.02 V (vs. SCE) due to the enhanced electron density by introducing anthracenyl group, which is proved by the calculation results that the HOMO of anthracene gets delocalized over the BODIPY.[53] Compound **5** shows one reversible oxidation potential (1.31 V vs. SCE) and three reversible reduction potentials (-0.93, -1.18, -1.49 V vs. SCE). Compound **6** shows one reversible oxidation potential (1.29 V vs. SCE) and three reversible reduction potentials (-0.92, -1.28, -1.48 V vs. SCE). The first and the third reduction potentials of compound **5** (-0.93 and -1.49 V) and compound **6** (-0.92 and -1.48 V) belong to the anthraquinonyl moiety. The second reduction potentials of compound **5** (-1.18 V) and compound **6** (-1.28 V) belong to the BODIPY core. Compared to compound **1**, the oxidation potential of BODIPY core for compound **5** and compound **6** (1.31 and 1.29) all migrate positively, indicating a harder oxidation requirement. The reason for this is that the LUMO+1 of compound **5** and LUMO+2 of compound **6** become delocalized over anthraquinone according to the calculation results.

The HOMO and LUMO energy levels and the energy gap of compounds **2-6** are evaluated from the cyclic voltammograms. The energy gap of compound **1** is reported to be 2.43 eV.[30] For compound **2**, according to the CV results, the energy gap is 2.40 eV. Thus, the introduction of the iodo group stabilizes the BODIPY core and narrows the energy gap. The HOMO level, the LUMO level and the energy gap for compound **3** are -5.66, -3.26 and 2.40 eV. Compared to compound **3**, compound **4** shows only slight changes on the HOMO level (-5.60 eV), the LUMO level (-3.19 eV) and the energy gap (2.41 eV). When it comes to compound **5**, the HOMO level, the LUMO level and the energy gap are -5.71, -3.47 and 2.24 eV. In comparison to compound **3**, the replacement of

anthracenyl by anthraquinonyl moiety in compound **5** markedly lowers the LUMO level by 0.21 eV (this value for the HOMO level is only 0.05 eV), which results a smaller energy gap. The HOMO level (-5.69 eV), the LUMO level (-3.48 eV) and the energy gap (2.21 eV) for compound **6** are very close to those of compound **5**.

3.6. TD-DFT calculations

For the BODIPY core, the intrinsic reason for the changes of photophysical and electrochemical properties is the inductive effect of the modifying groups on the frontier orbits.[54] To obtain the excited states and molecular orbital energy levels of compounds **3**-**6**, theoretical calculations were carried out by TD-DFT method at B3LYP/6-31tG* level.[43] (Table S6) For compound **3**, the absorption band located at 531 nm is attributed to HOMO→LUMO transition. (Table S7-1) The peak at 243 nm is attributed to HOMO→LUMO+3 transition, and these two molecular orbitals are situated at anthracenyl moiety, indicating this absorption band arises from the anthracenyl unit. (Figure S6) The peak at 384 nm is attributed to HOMO-2→LUMO transition. Because HOMO-2 orbital is mainly situated at anthracenyl unit, while LUMO orbital is situated at BODIPY core, this transition is a typical ICT process from the anthracenyl moiety to the BODIPY core. For compound **4**, the absorption band located around 524 nm is attributed to HOMO→LUMO transition. (Table S7-2) The peak at 278 nm is attributed to HOMO→LUMO+3 transition, also arising from anthracenyl unit. The peak at 382 nm is attributed to HOMO-3→LUMO transition, which is also an ICT process from the anthracenyl moiety to the BODIPY core. For compound **5**, the absorption band located around 511 nm is attributed to HOMO→LUMO transition. (Table S7-3) The peak at 280 nm is attributed to HOMO-1→LUMO+2 transition, and the peak at 388 nm is attributed to HOMO-1→LUMO transition, and these two transitions are all ICT process from

the BODIPY core to the anthraquinonyl moiety. For compound **6**, the absorption band located around 518 nm is attributed to HOMO→LUMO transition. (Table S7-4) The peak at 381 nm is attributed to HOMO-1→LUMO+2 transition, which is also an ICT process from the BODIPY core to the anthraquinonyl moiety.

4. Conclusions

In summary, a series of anthracenyl(anthraquinonyl)-substituted BODIPY dyes have been designed and synthesized based on Suzuki cross-coupling reactions. Photophysical characterization combined with electrochemical characterization demonstrates that anthracenyl(anthraquinonyl) fragment effectively alters the emission and electrical properties while maintaining the absorption properties. The geometry optimization by Gaussian calculation matches well with the crystallographic data. Theoretical calculation on the excited states and molecular orbital energy levels of these compounds are also conducted. The results suggest that a moderate intramolecular charge-transfer process from the anthracenyl moiety to the BODIPY core occurs in compounds **3** and **4**, while intramolecular charge-transfer process from the BODIPY core to the anthraquinonyl moiety happened in compounds **5** and **6**. These characterizations of anthracenyl(anthraquinonyl)-substituted BODIPY dyes should help in development of new dyes for future applications.

Acknowledgement

This work was supported by the National Nature Science Foundation of China (21031006, 21290190 and 21322301), NSFC-DFG joint fund (TRR 61) and the National Basic Research 973 Program of China (2011CB932302 and 2012CB932900).

References

[1] Karolin J, Johansson LBA, Strandberg L, Ny T. Fluorescence and absorption spectroscopic properties of dipyrrometheneboron difluoride (BODIPY) derivatives in liquids, lipid membranes, and proteins. J Am Chem Soc 1994; 116:7801-6.

[2] Sculimbrene BR, Imperiali B. Lanthanide-binding tags as luminescent probes for studying protein interactions. J Am Chem Soc 2006; 128:7346-52.

[3] Rurack K, Kollmannsberger M, Resch-Genger U, Daub J. A selective and sensitive fluoroionophore for HgII, AgI, and CuII with virtually decoupled fluorophore and receptor units. J Am Chem Soc 2000; 122:968-9.

[4] Yamada K, Nomura Y, Citterio D, Iwasawa N, Suzuki K. Highly sodium-selective fluoroionophore based on conformational restriction of oligoethyleneglycol-bridged biaryl boron−dipyrromethene. J Am Chem Soc 2005; 127:6956-7.

[5] Coskun A, Akkaya EU. Ion sensing coupled to resonance energy transfer: a highly selective and sensitive ratiometric fluorescent chemosensor for Ag(I) by a modular approach. J Am Chem Soc 2005; 127:10464-5.

[6] Bricks JL, Kovalchuk A, Trieflinger C, Nofz M, Büschel M, Tolmachev AI et al. On the development of sensor molecules that display FeIII-amplified fluorescence. J Am Chem Soc 2005; 127:13522-9.

[7] Zeng L, Miller EW, Pralle A, Isacoff EY, Chang CJ. A selective turn-on fluorescent sensor for imaging copper in living cells. J Am Chem Soc 2005; 128:10-1.

[8] Boens N, Leen V, Dehaen W. Fluorescent indicators based on BODIPY. Chem Soc Rev 2012; 41:1130-72.

[9] Trieflinger C, Rurack K, Daub J. "Turn ON/OFF your LOV light": Borondipyrromethene–flavin dyads as biomimetic switches derived from the LOV domain. Angew Chem Int Ed 2005; 44:2288-91.

[10] Golovkova TA, Kozlov DV, Neckers DC. Synthesis and properties of novel fluorescent switches. J Org Chem 2005; 70:5545-9.

[11] Arbeloa TL, Arbeloa FL, Arbeloa IL, García-Moreno I, Costela A, Sastre R et al. Correlations between photophysics and lasing properties of dipyrromethene–BF2 dyes in solution. Chem Phys Lett 1999; 299:315-21.

[12] McCusker C, Carroll JB, Rotello VM. Cationic polyhedral oligomeric silsesquioxane (POSS) units as carriers for drug delivery processes. Chem Commun 2005; 0:996-8.

[13] Lai RY, Bard AJ. Electrogenerated chemiluminescence 71. Photophysical, electrochemical, and electrogenerated chemiluminescent properties of selected dipyrromethene−BF2 dyes. J Phys Chem B 2003; 107:5036-42.

[14] Hattori S, Ohkubo K, Urano Y, Sunahara H, Nagano T, Wada Y et al. Charge separation in a nonfluorescent donor−acceptor dyad derived from boron dipyrromethene dye, leading to photocurrent generation. J Phys Chem B 2005; 109:15368-75.

[15] Erten-Ela S, Yilmaz MD, Icli B, Dede Y, Icli S, Akkaya EU. A panchromatic boradiazaindacene (BODIPY) sensitizer for dye-sensitized solar cells. Org Lett 2008; 10:3299-302.

[16] Ulrich G, Ziessel R, Harriman A. The chemistry of fluorescent Bodipy dyes: versatility unsurpassed. Angew Chem Int Ed 2008; 47:1184-201.

[17] Kee HL, Kirmaier C, Yu L, Thamyongkit P, Youngblood WJ, Calder ME et al. Structural control of the photodynamics of boron−dipyrrin complexes. J Phys Chem B 2005; 109:20433-43.

[18] Loudet A, Burgess K. BODIPY dyes and their derivatives: syntheses and spectroscopic properties. Chem Rev 2007; 107:4891-932.

[19] Kim TG, Castro JC, Loudet A, Jiao JGS, Hochstrasser RM, Burgess K et al. Correlations of structure and rates of energy transfer for through-bond energy-transfer cassettes. J Phys Chem A 2005; 110:20-7.

[20] Wan CW, Burghart A, Chen J, Bergström F, Johansson LBA, Wolford MF et al. Anthracene–BODIPY cassettes: syntheses and energy transfer. Chem Eur J 2003; 9:4430-41.

[21] Burghart A, Kim H, Welch MB, Thoresen LH, Reibenspies J, Burgess K et al. 3,5-Diaryl-4,4-difluoro-4-bora-3a,4a-diaza-s-indacene (BODIPY) dyes: synthesis, spectroscopic, electrochemical, and structural properties. J Org Chem 1999; 64:7813-9.

[22] Niu S, Ulrich G, Retailleau P, Ziessel R. BODIPY-bridged push–pull chromophores: optical and electrochemical properties. Tetrahedron Lett 2011; 52:4848-53.

[23] Dimitrakopoulos CD, Malenfant PRL. Organic thin film transistors for large area electronics. Adv Mater 2002; 14:99-117.

[24] Ito K, Suzuki T, Sakamoto Y, Kubota D, Inoue Y, Sato F et al. Oligo(2,6-anthrylene)s: acene–oligomer approach for organic field-effect transistors. Angew Chem Int Ed 2003; 42:1159-62.

[25] Li Y, Xu L, Liu T, Yu Y, Liu H, Li Y et al. Anthraceno-perylene bisimides: the precursor of a new acene. Org Lett 2011; 13:5692-5.

[26] Xu L, Liu C, Qin Z, Jiang R, Li Y. Core expansion of perylenetetracarboxdiimide dyes with anthraquinone units for electron-accepting materials. Eur J Org Chem 2013; 2013:300-6.

[27] Wilkinson F. Transfer of Triplet state energy and the chemistry of excited states. J Phys Chem 1962; 66:2569-74.

[28] Görner H. Photoreduction of 9,10-anthraquinone derivatives: transient spectroscopy and effects of alcohols and amines on reactivity in solution. Photochem Photobiol 2003; 77:171-9.

[29] Kollmannsberger M, Rurack K, Resch-Genger U, Daub J. Ultrafast charge transfer in amino-substituted boron dipyrromethene dyes and its inhibition by cation complexation: a new design concept for highly sensitive fluorescent probes. J Phys Chem A 1998; 102:10211-20.

[30] Nepomnyashchii AB, Bröring M, Ahrens J, Bard AJ. Synthesis, photophysical, electrochemical, and electrogenerated chemiluminescence studies. Multiple sequential electron transfers in BODIPY monomers, dimers, trimers, and polymer. J Am Chem Soc 2011; 133:8633-45.

[31] Fu L, Jiang F-L, Fortin D, Harvey PD, Liu Y. A reaction-based chromogenic and fluorescent chemodosimeter for fluoride anions. Chem Commun 2011; 47:5503-5.

[32] Boens N, Leen V, Dehaen W, Wang L, Robeyns K, Qin W et al. Visible absorption and fluorescence spectroscopy of conformationally constrained, annulated BODIPY dyes. J Phys Chem A 2012; 116:9621-31.

[33] Leen V, Leemans T, Boens N, Dehaen W. 2- and 3-Monohalogenated BODIPY dyes and their functionalized analogues: synthesis and spectroscopy. Eur J Org Chem 2011; 2011:4386-96.

[34] Leen V, Miscoria D, Yin S, Filarowski A, Molisho Ngongo J, Van der Auweraer M et al. 1,7-Disubstituted boron dipyrromethene (BODIPY) dyes: synthesis and spectroscopic properties. J Org Chem 2011; 76:8168-76.

[35] Leen V, Braeken E, Luckermans K, Jackers C, Van der Auweraer M, Boens N et al. A versatile, modular synthesis of monofunctionalized BODIPY dyes. Chem Commun 2009:4515-7.

[36] Baruah M, Qin W, Basarić N, De Borggraeve WM, Boens N. BODIPY-based hydroxyaryl derivatives as fluorescent pH probes. J Org Chem 2005; 70:4152-7.

[37] Fron E, Coutino-Gonzalez E, Pandey L, Sliwa M, Van der Auweraer M, De Schryver FC et al. Synthesis and photophysical characterization of chalcogen substituted BODIPY dyes. New J Chem 2009; 33:1490-6.

[38] Ziessel R, Ulrich G, Harriman A. The chemistry of Bodipy: A new El Dorado for fluorescence tools. New J Chem 2007; 31:496-501.

[39] Hankache J, Wenger OS. Microsecond charge recombination in a linear triarylamine-Ru(bpy)$_3^{2+}$-anthraquinone triad. Chem Commun 2011; 47:10145-7.

[40] Thalladi VR, Weiss H-C, Bläser D, Boese R, Nangia A, Desiraju GR. C−H···F interactions in the crystal structures of some fluorobenzenes. J Am Chem Soc 1998; 120:8702-10.

[41] Ziessel R, Goze C, Ulrich G, Césario M, Retailleau P, Harriman A et al. Intramolecular energy transfer in pyrene–Bodipy molecular dyads and triads. Chem Eur J 2005; 11:7366-78.

[42] Madhu S, Rao MR, Shaikh MS, Ravikanth M. 3,5-Diformylboron dipyrromethenes as fluorescent pH sensors. Inorg Chem 2011; 50:4392-400.

[43] Frisch MJ, Trucks GW, Schlegel HB, Scuseria GE, Robb MA, Cheeseman JR et al. Gaussian 03, Revision C.02.

[44] Sooambar C, Troiani V, Bruno C, Marcaccio M, Paolucci F, Listorti A et al. Synthesis, photophysical, electrochemical, and electrochemiluminescent properties of 5,15-bis(9-anthracenyl)porphyrin derivatives. Org Biomol Chem 2009; 7:2402-13.

[45] Yang J, Dass A, Rawashdeh A-MM, Sotiriou-Leventis C, Panzner MJ, Tyson DS et al. Arylethynyl substituted 9,10-anthraquinones: tunable stokes shifts by substitution and solvent polarity. Chem Mater 2004; 16:3457-68.

[46] de Silva AP, Gunaratne HQN, Gunnlaugsson T, Huxley AJM, McCoy CP, Rademacher JT et al. Signaling recognition events with fluorescent sensors and switches. Chem Rev 1997; 97:1515-66.

[47] Williams ATR, Winfield SA, Miller JN. Relative fluorescence quantum yields using a computer-controlled luminescence spectrometer. Analyst 1983; 108:1067-71.

[48] Olmsted J. Calorimetric determinations of absolute fluorescence quantum yields. J Phys Chem 1979; 83:2581-4.

[49] Fischer M, Georges J. Fluorescence quantum yield of rhodamine 6G in ethanol as a function of concentration using thermal lens spectrometry. Chem Phys Lett 1996; 260:115-8.

[50] de Leeuw DM, Simenon MMJ, Brown AR, Einerhand REF. Stability of n-type doped conducting polymers and consequences for polymeric microelectronic devices. Synth Met 1997; 87:53-9.

[51] Li Y, Cao Y, Gao J, Wang D, Yu G, Heeger AJ. Electrochemical properties of luminescent polymers and polymer light-emitting electrochemical cells. Synth Met 1999; 99:243-8.

[52] Yogo T, Urano Y, Ishitsuka Y, Maniwa F, Nagano T. Highly efficient and photostable photosensitizer based on BODIPY chromophore. J Am Chem Soc 2005; 127:12162-3.

[53] Ando S, Nishida JI, Fujiwara E, Tada H, Inoue Y, Tokito S et al. Novel p- and n-type organic semiconductors with an anthracene unit. Chem Mater 2005; 17:1261-4.

[54] Yin X, Li Y, Zhu Y, Kan Y, Li Y, Zhu D. Synthesis of a pentalene centered polycyclic fused system. Org Lett 2011; 13:1520-3.

Figure Captions

Scheme 1. Synthesis route for compounds **3-6**. Conditions: a) DMF, Ar_2, 2-anthracen-2-yl-4,4,5,5-tetramethyl-[1,3,2]dioxaborolane, K_2CO_3, Pd $(Ph_3P)_4$, 80°C, 12 h, b) the same as above except for the replacement of 2-anthracen-2-yl-4,4,5,5-tetramethyl-[1,3,2]dioxaborolane by 2-anthraquinon-2-yl-4,4,5,5-tetramethyl-[1,3,2]dioxaborolane.

Figure 1. The crystal structures of compounds **1** (a) and **7** (d), the crystal packing diagrams of compound **1** (b) and **7** (e) in one crystal cell and those of compound **1** (c) and **7** (f) along different axis.

Figure 2. Calculated geometric structures (a, d, g, j) and frontier orbitals (b, e, h, k for HOMO, c, f, i, l for LUMO) of compounds **3-6**.

Figure 3. UV-vis absorption and fluorescence emission spectra of compounds **3-6** in CH_2Cl_2.

Figure 4. Cyclic voltammograms of compounds **2-6** vs SCE in CH_2Cl_2.

Table 1. Photophysical and electrochemical data for compounds **2-6**

Compound	**2**	**3**	**4**	**5**	**6**
Abs[a] λ_{max} [nm]	530[h]	532	536	532	532
ε[a] [$M^{-1}\cdot cm^{-1}$]	71323	85893	60268	70670	93199
Fluor[b] λ_{max} [nm]	546[h]	569	590	550	555
Φ_{fl}[c](%)	7.0[h]	6.5	70.3	0.3	0.3
Stokes shift[cm^{-1}]	552[h]	1222	1707	615	779
E_{ox} [V vs SCE][d]	1.49[e]	1.26[f], 1.54[f]	1.20[f], 1.58[f]	1.31[e]	1.29[e]
E_{red} [V vs SCE][d]	–0.91[e]	–1.14[e]	–1.21[e]	–0.93[e], –1.18[e], –1.49[e]	–0.92[e], –1.28[e], –1.48[e]
HOMO/LUMO [eV][g]	–5.89/–3.49	–5.66/–3.26	–5.60/–3.19	–5.71/–3.47	–5.69/–3.48
E_g [eV][g]	2.40	2.40	2.41	2.24	2.21

[a]. Measured in CH_2Cl_2 solution (1.0×10^{-5} M). [b]. Measured in CH_2Cl_2 solution (1.0×10^{-6} M), upon excitation at 465 nm (compound **1**), 500 nm (compound **2**), and 510 nm (compound **3-6**). [c]. In CH_2Cl_2, rodamin 6G, Φ_{fl} = 0.76 in H_2O[47-49] as the standard. [d]. Performing in CH_2Cl_2, in a N_2 atmosphere, using nBu_4NPF_6 (0.05 M) as the supporting electrolyte, platinum as the counter electrode, glassy carbon as the work electrode and the saturated calomel electrode (SCE) as the reference electrode. [e]. Half-wave potential (reversible). [f]. peak potential (irreversible) [g]. HOMO, LUMO and E_g levels are obtained directly from CV according to the method reported in the literature.[50, 51] [h]. Values are reported in reference 31.

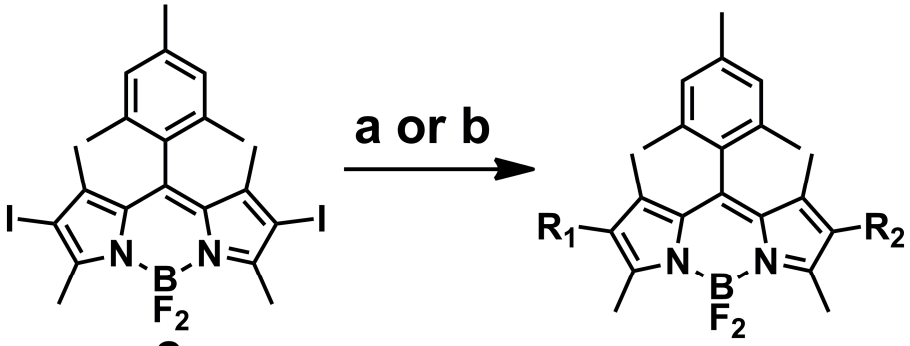

2

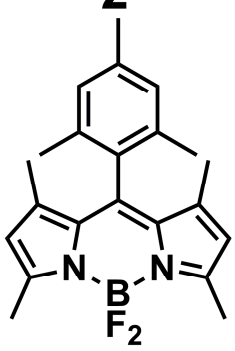

1

3 R_1=2-anthracenyl, R_2=iodine
4 R_1=R_2=2-anthracenyl
5 R_1=2-anthraquinonyl, R_2=iodine
6 R_1=R_2=2-anthraquinonyl
7 R_1=2-anthraquinonyl, R_2=hydrogen

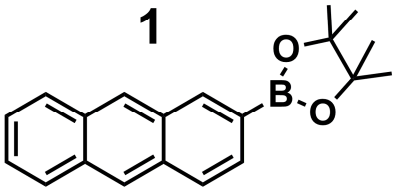

2-anthracen-2-yl-
4,4,5,5-tetramethyl-
[1,3,2]dioxaborolane

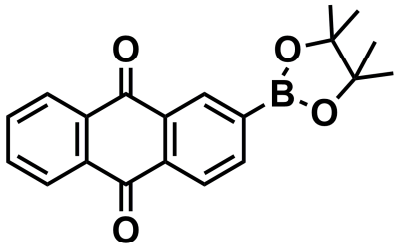

2-anthraquinon-2-yl-
4,4,5,5-tetramethyl-
[1,3,2]dioxaborolane

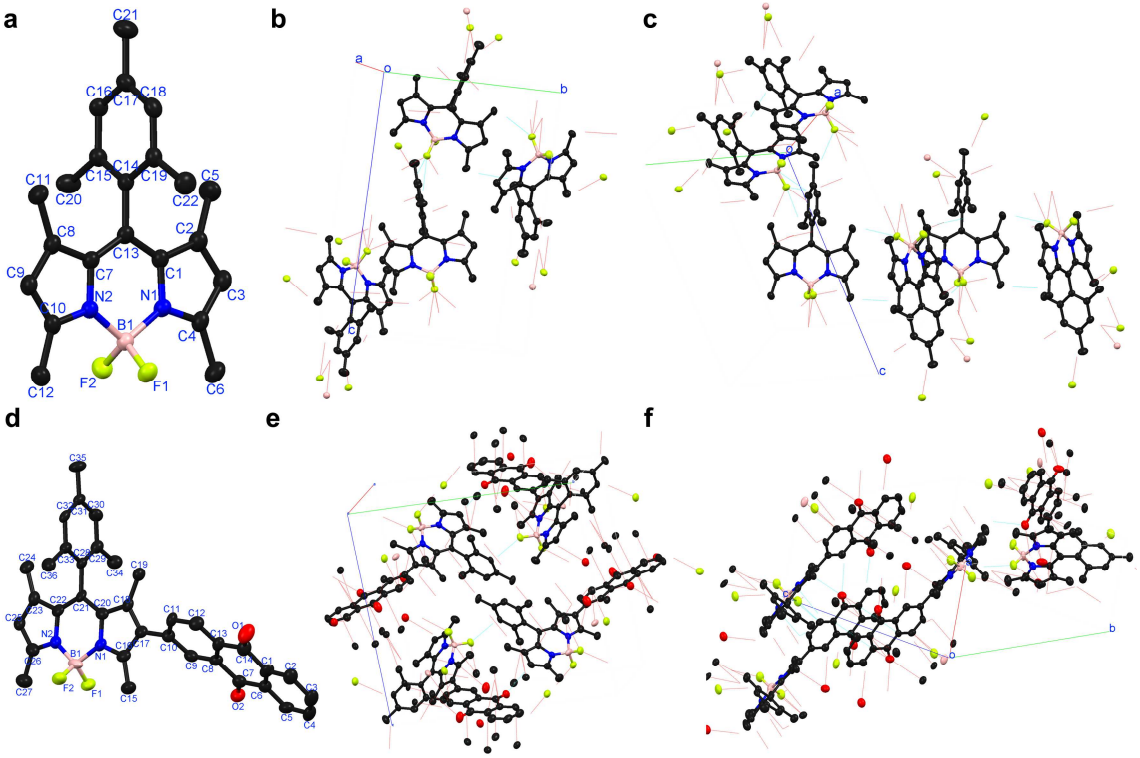

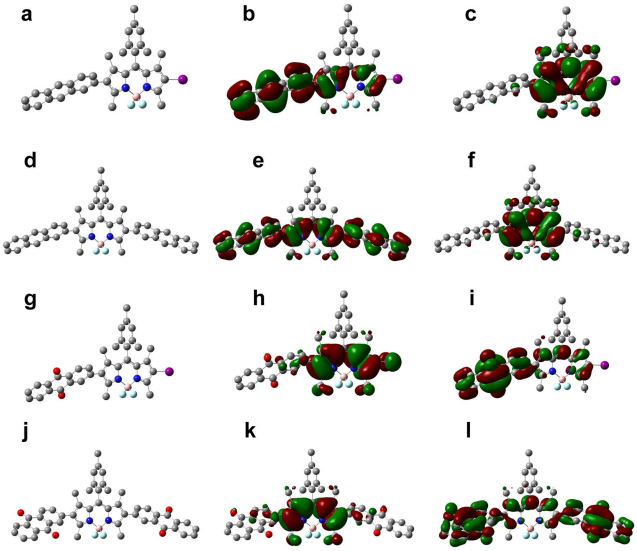

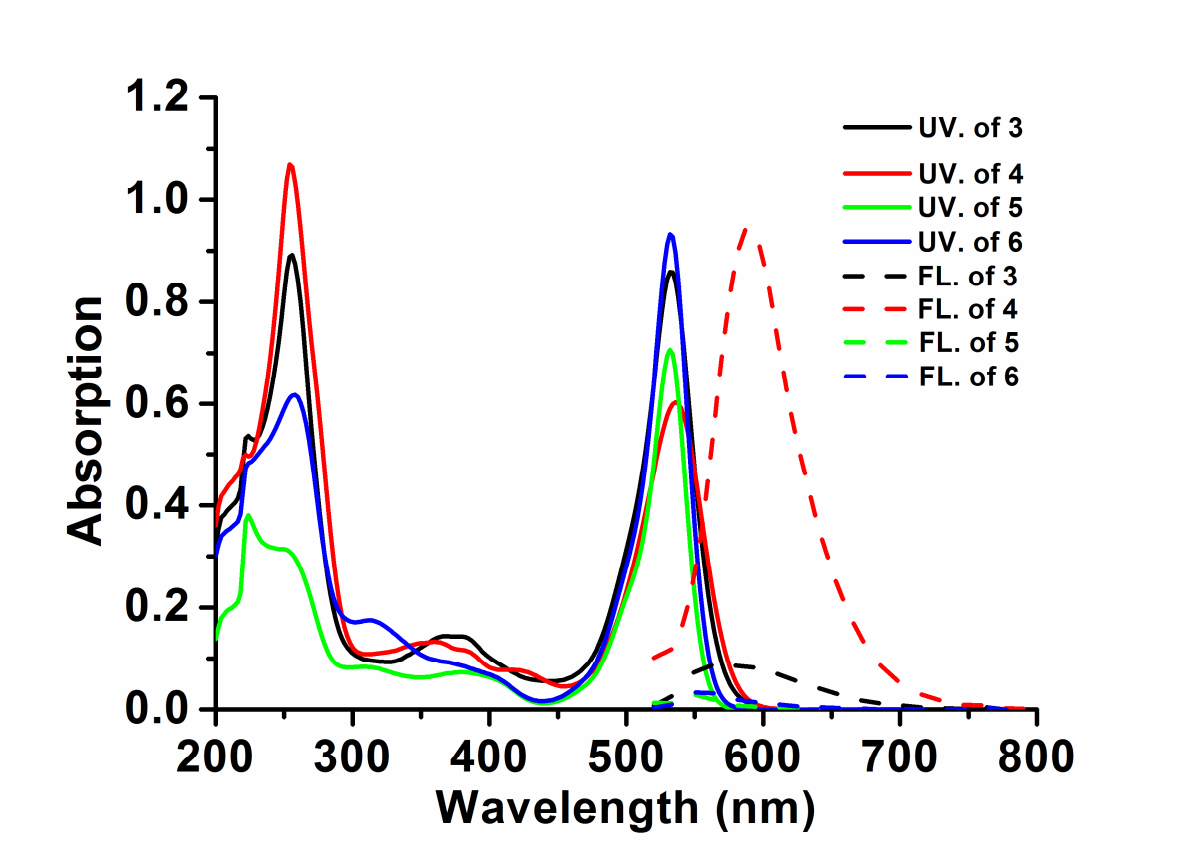

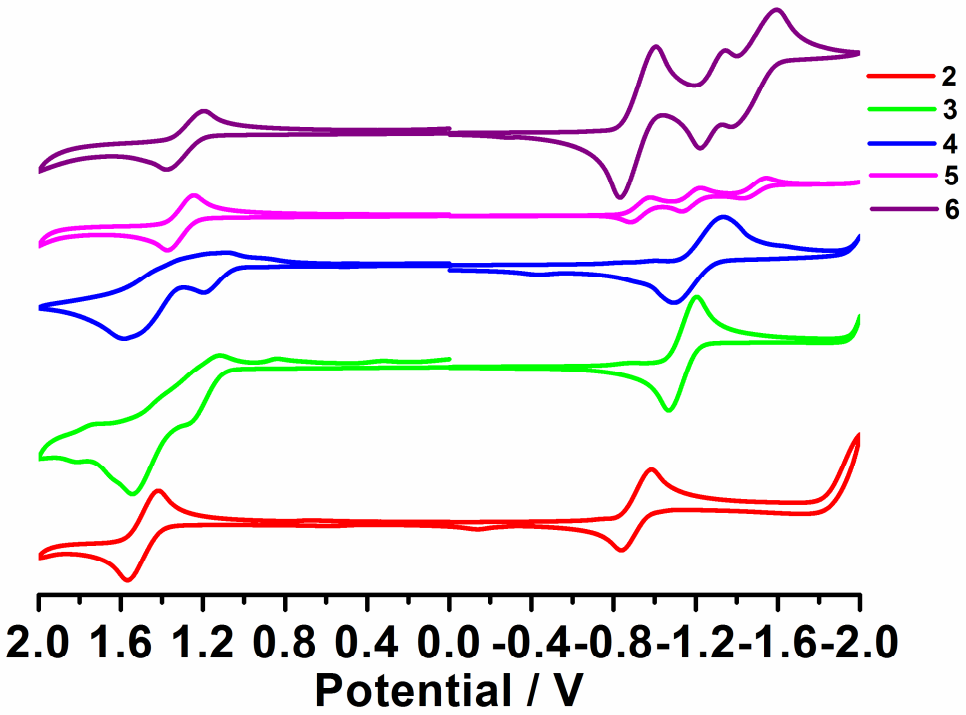

- A series of anthracenyl (anthraquinonyl)-substituted Bodipy dyes are synthesized.
- Moderate dihedral angles exist in anthracenyl (anthraquinonyl) and pyrrolyl plane.
- Rich and tunable emission and electrical properties are obtained.
- ICT process is proved between Bodipy core and anthracenyl (anthraquinonyl) moiety.

Supporting Information

2,6-anthracenyl(anthraquinonyl)-substituted Difluoroboron Dipyrromethene: Synthesis, Spectroscopy, Electrochemistry and Quantum Chemical Calculations

Liang Xu,[†‡] *Yongjun Li**[†] *Runsheng Jiang,*[†‡] *Zhihong Qin,*[†‡] *Yuliang Li**[†]

†Beijing National Laboratory for Molecular Sciences (BNLMS), CAS Key Laboratory of Organic Solids, Institute of Chemistry, Chinese Academy of Sciences, Beijing 100190, P.R. China

‡University of Chinese Academy of Sciences, Beijing 100049, P.R. China

E-mail: liyj@iccas.ac.cn;

Table of contents

S7. Calculated absorption wavelengths and oscillator strength of compounds **3-6**

S1. Spectroscopic data

MALDI-TOF

For compound **3**

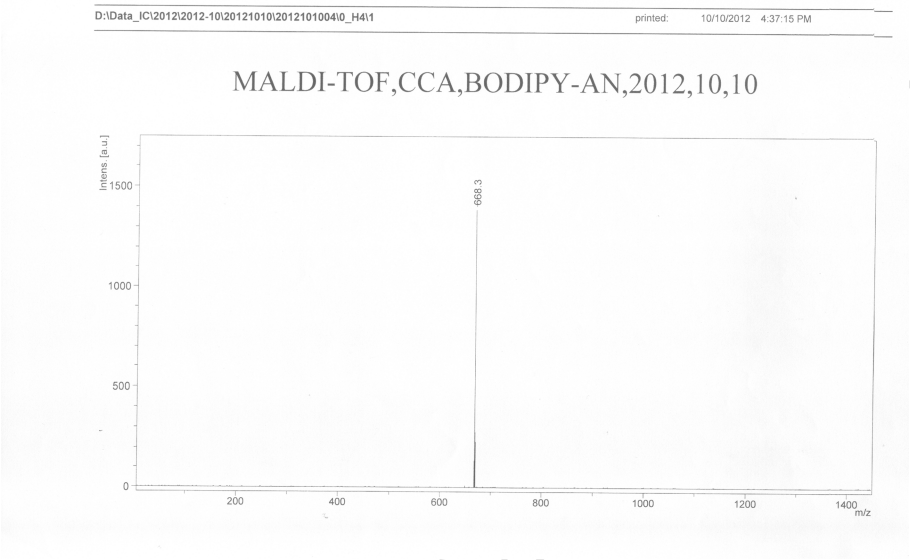

For compound **4**

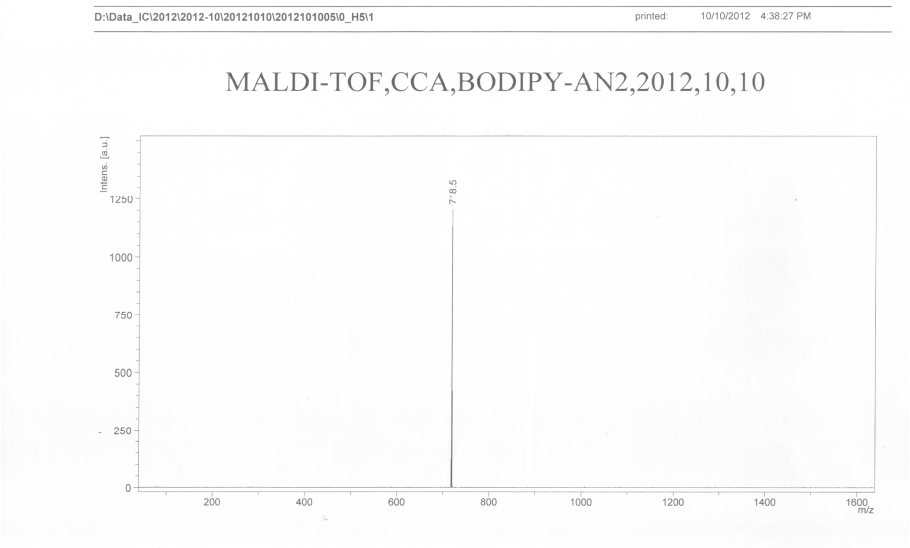

For compound **5**

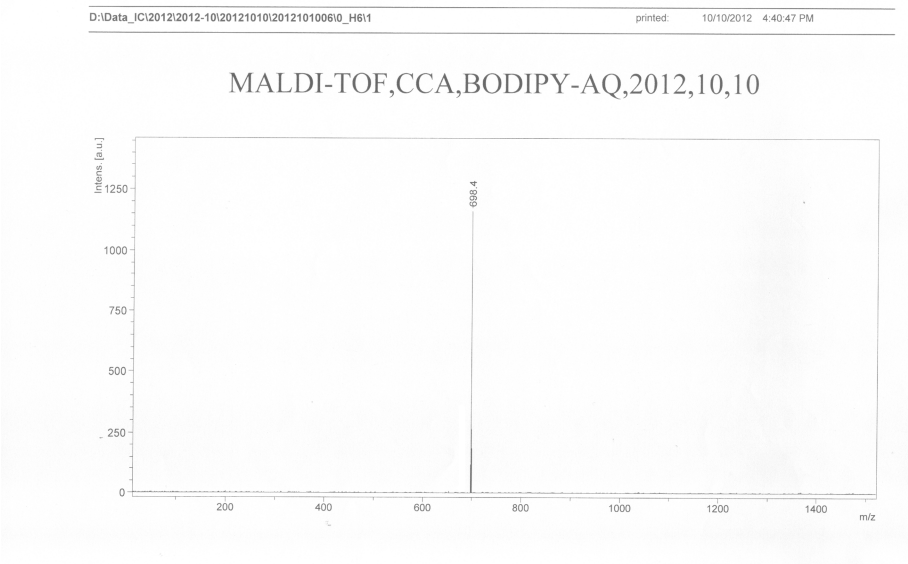

For compound **6**

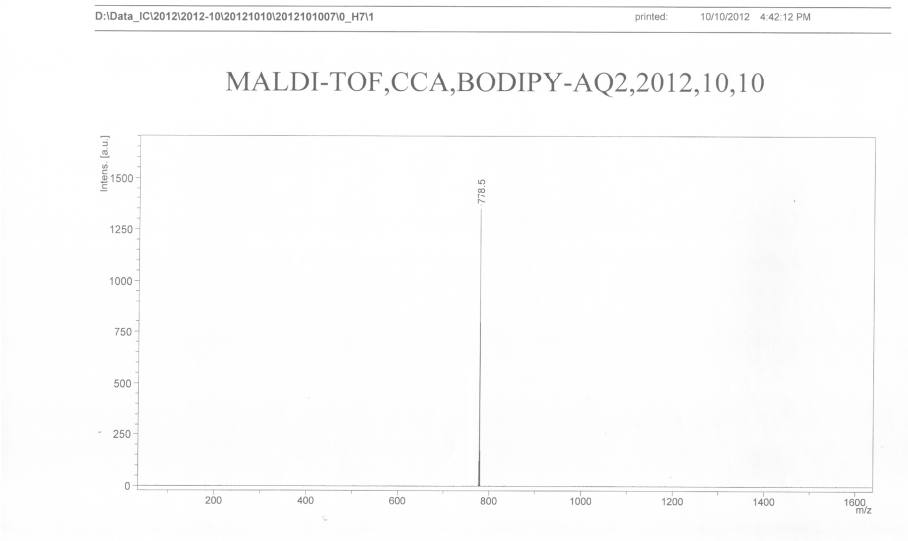

For compound **7**

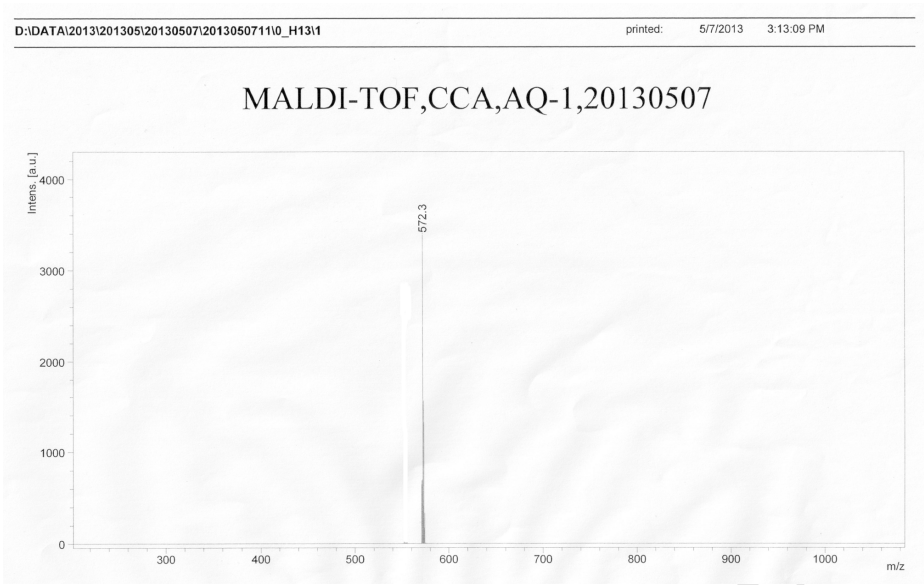

^{1}H NMR

For compound **3**

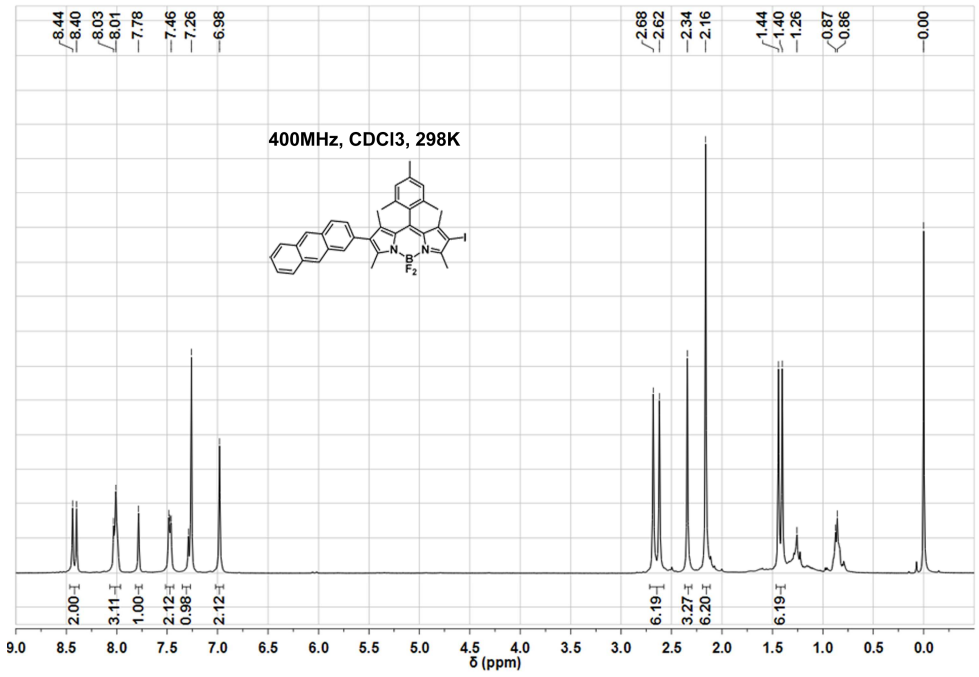

For compound **4**

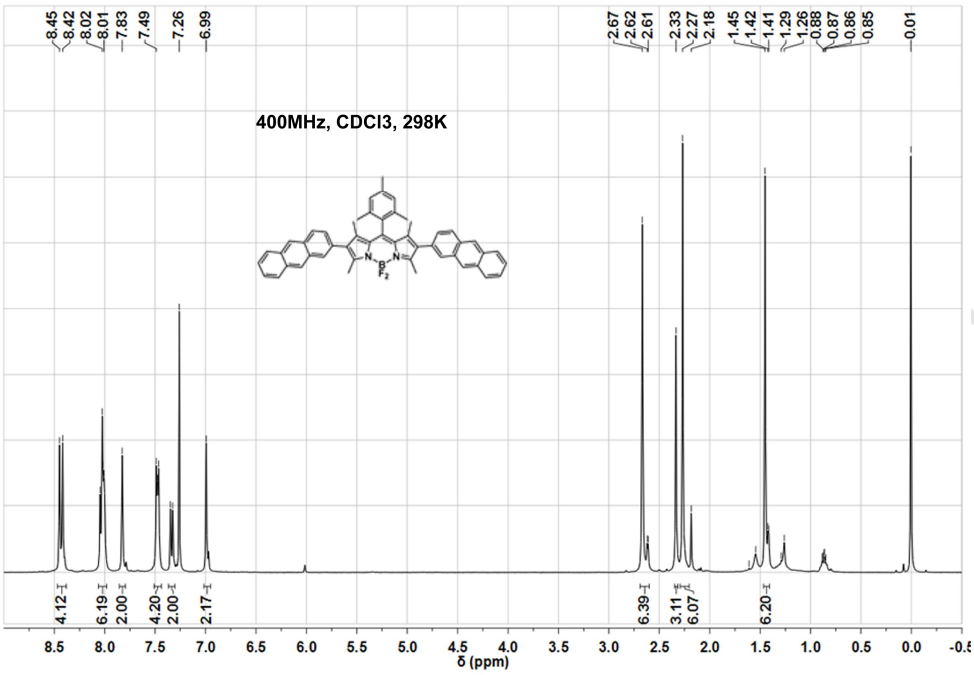

For compound **5**

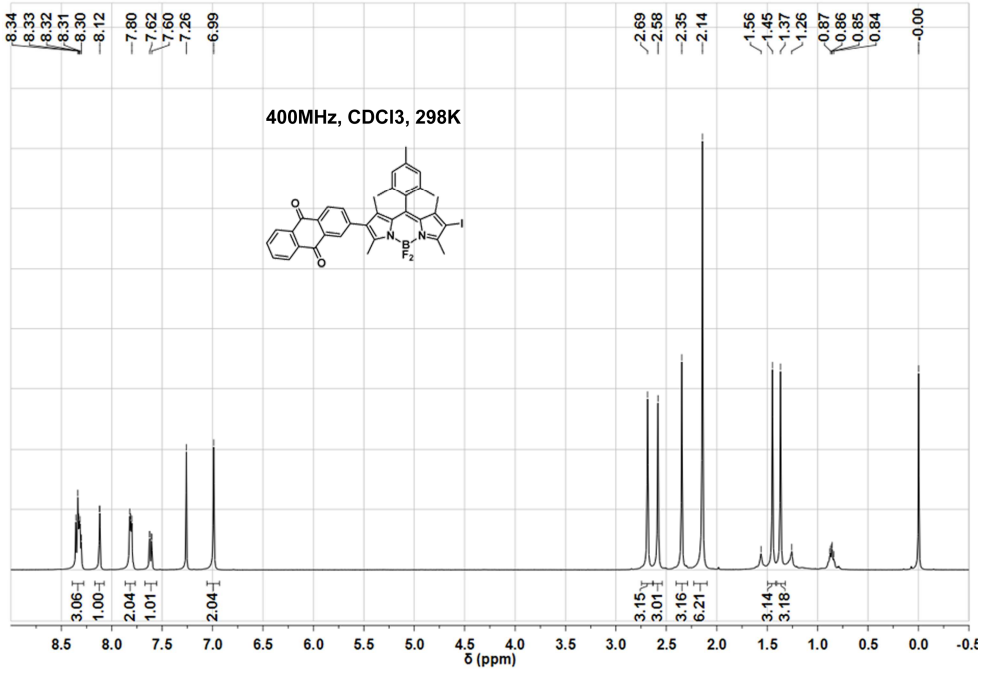

For compound **6**

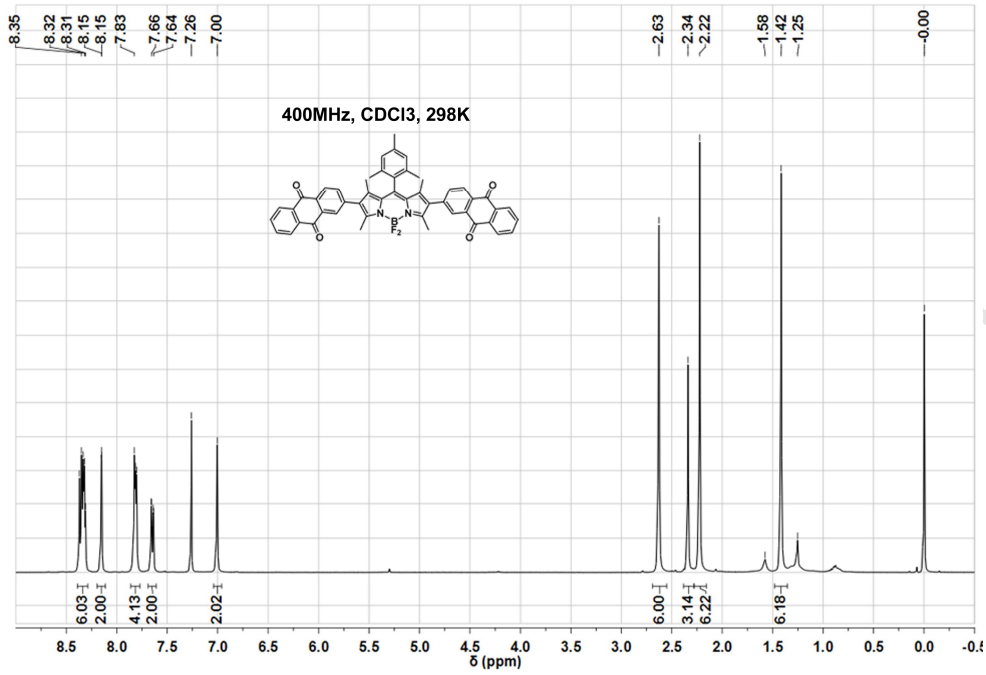

For compound **7**

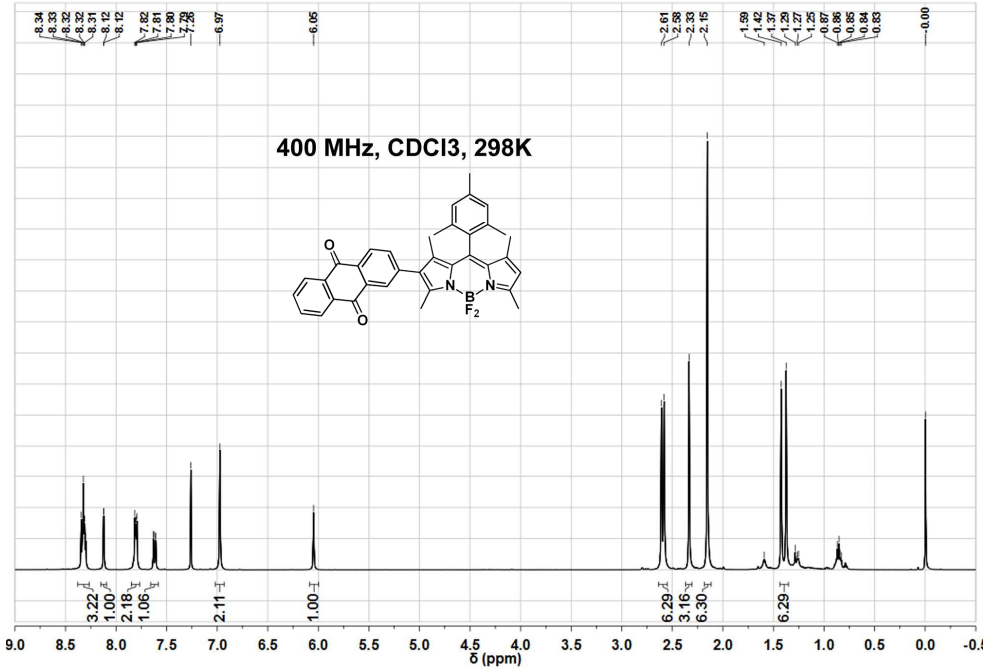

^{13}C NMR

For compound **3**

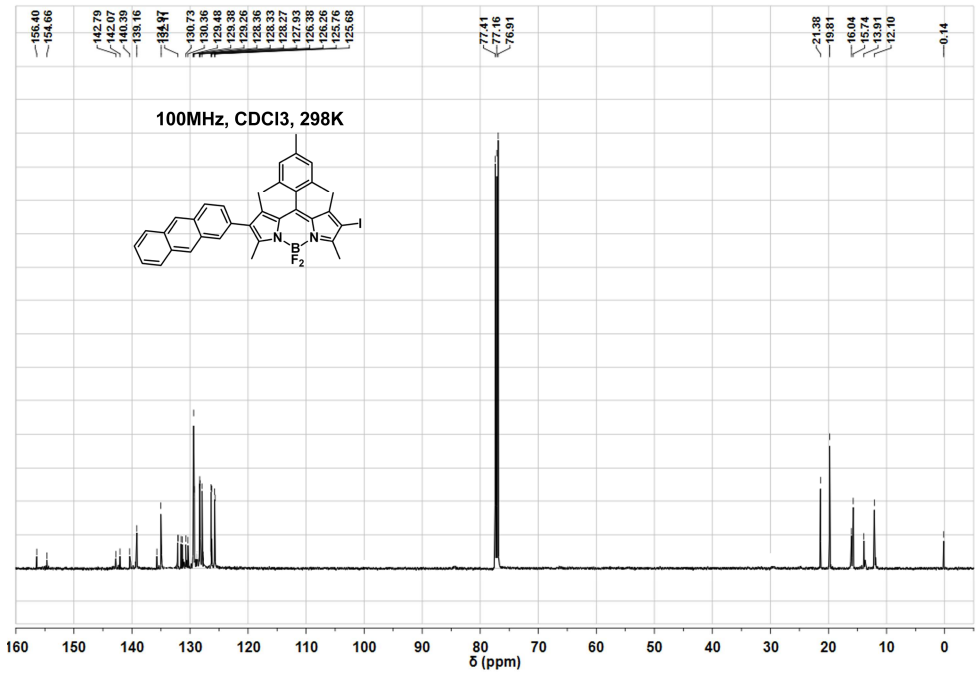

For compound **4**

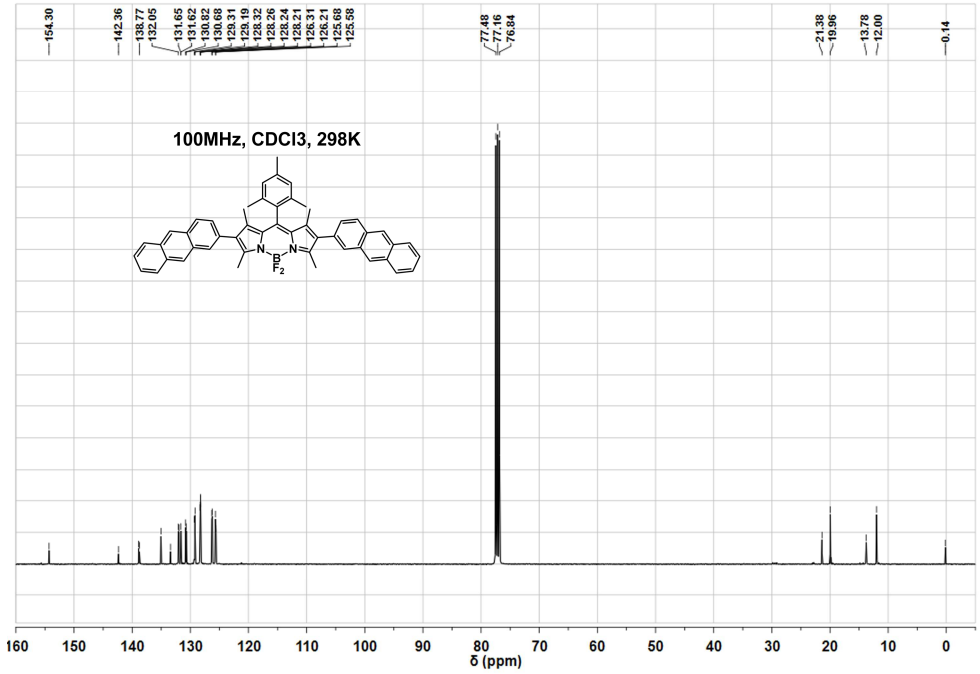

For compound **5**

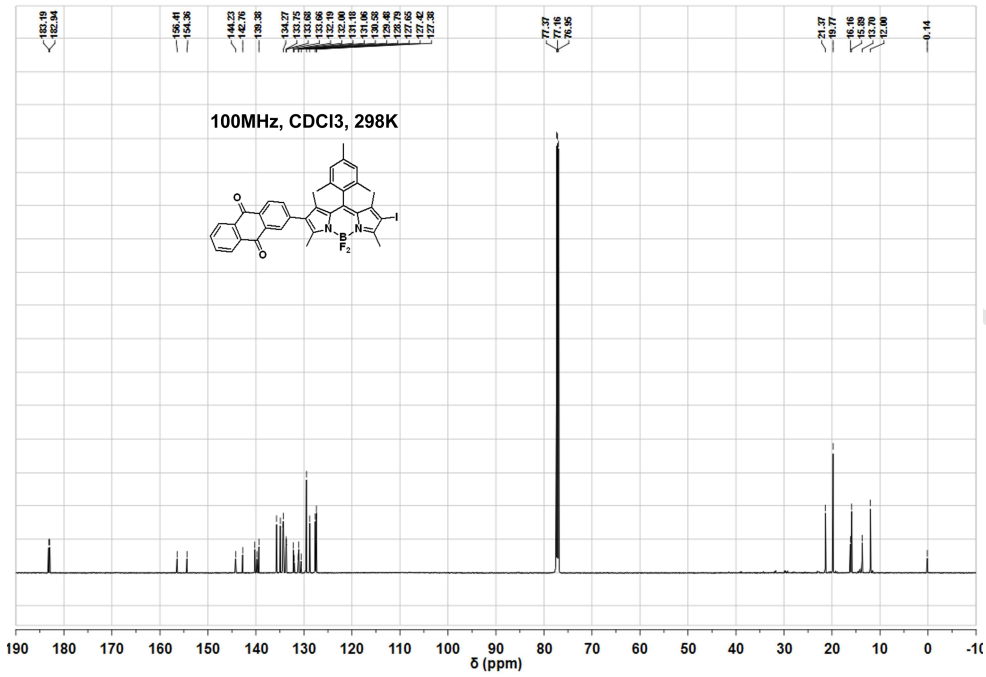

For compound **6**

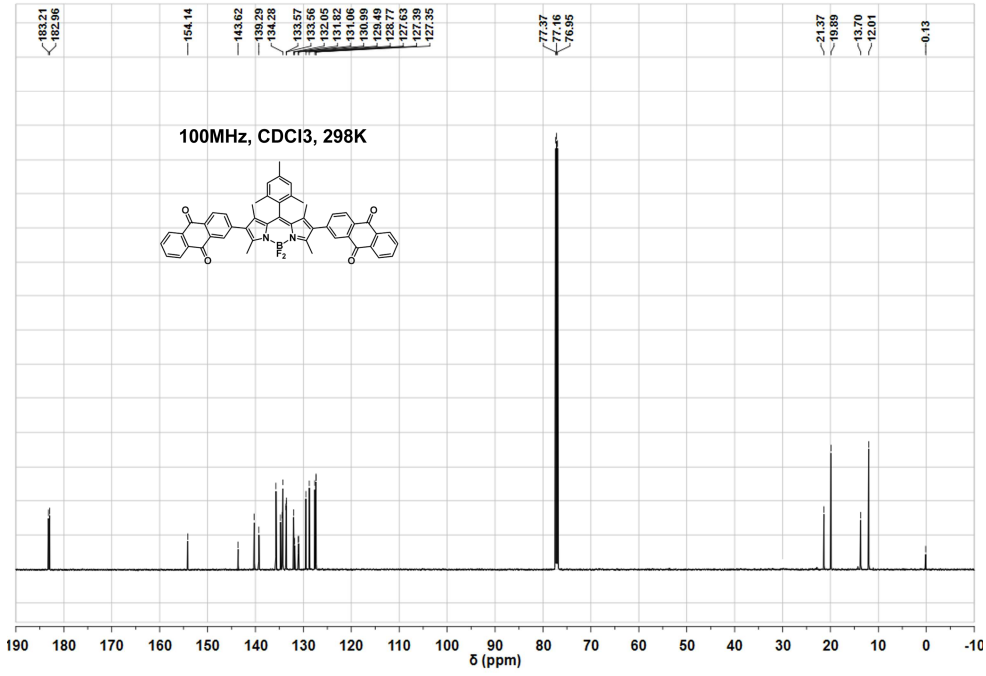

For compound **7**

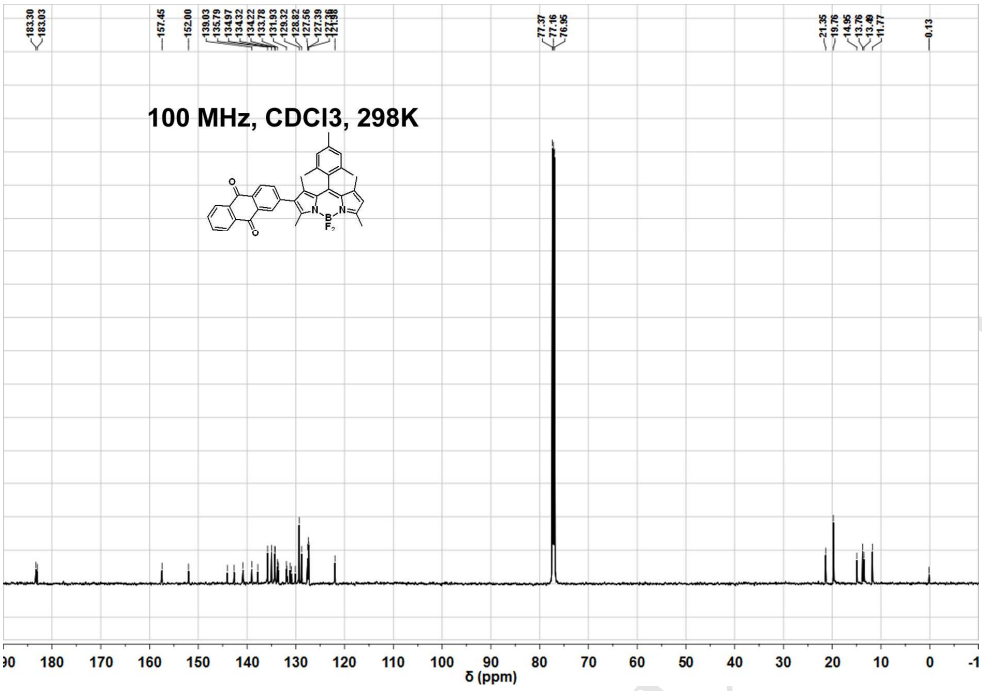

IR

For compound **3**

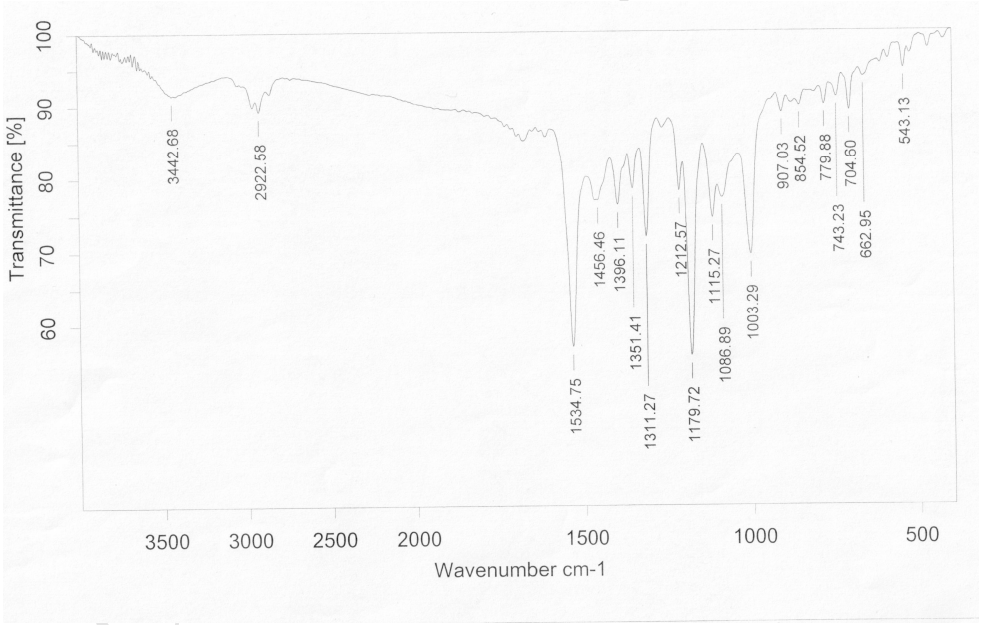

For compound **4**

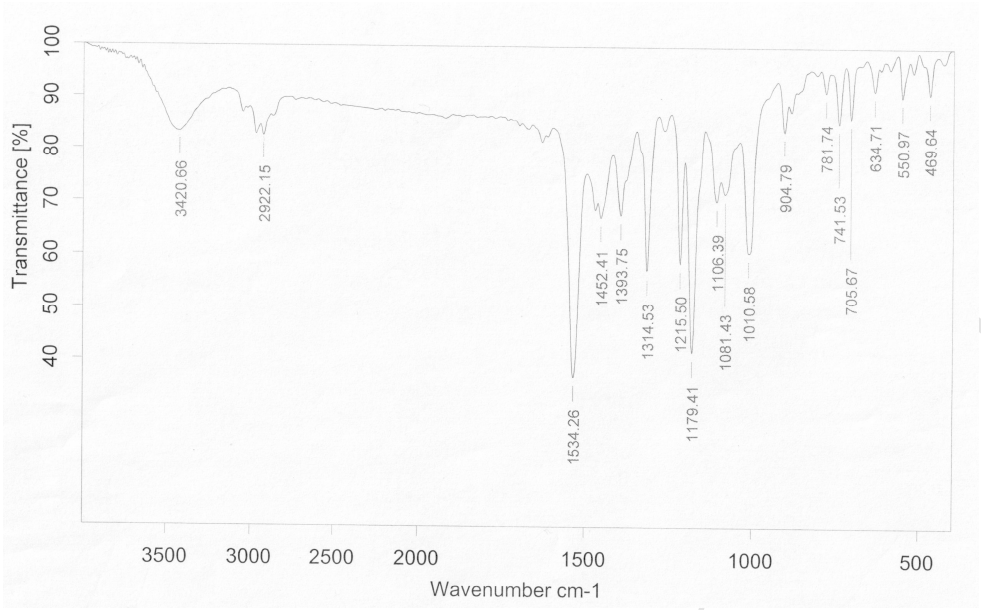

For compound **5**

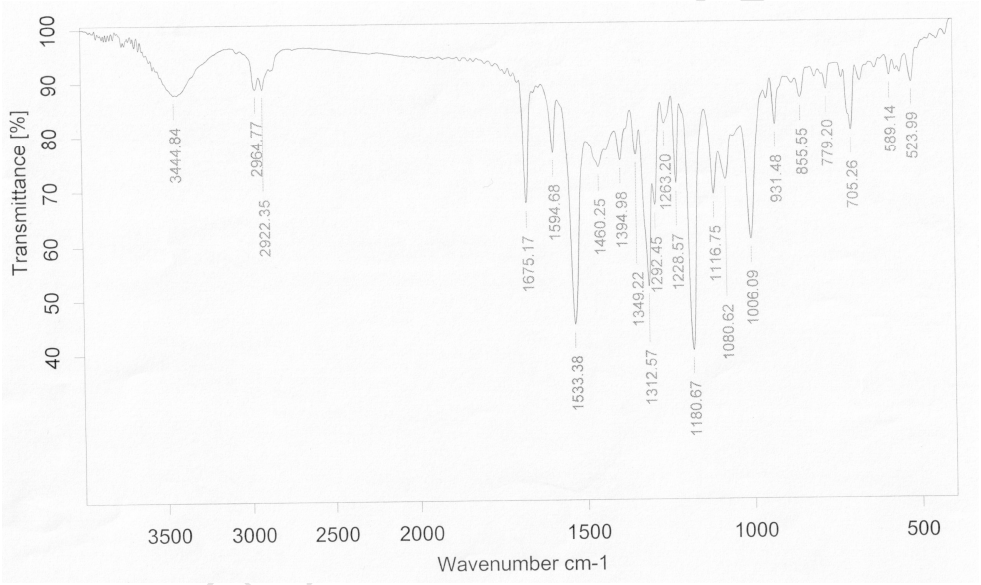

For compound **6**

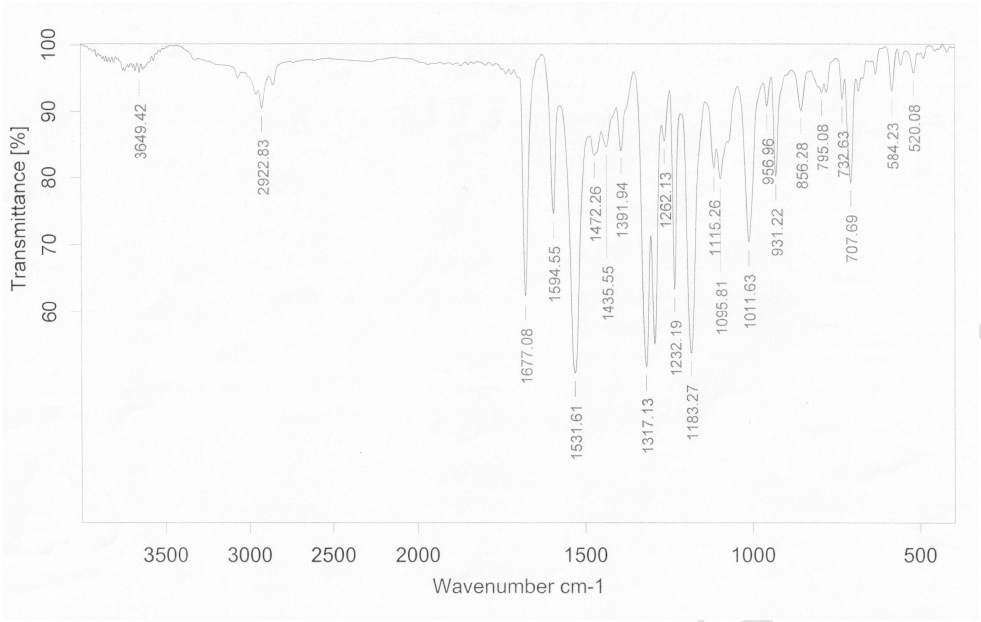

For compound **7**

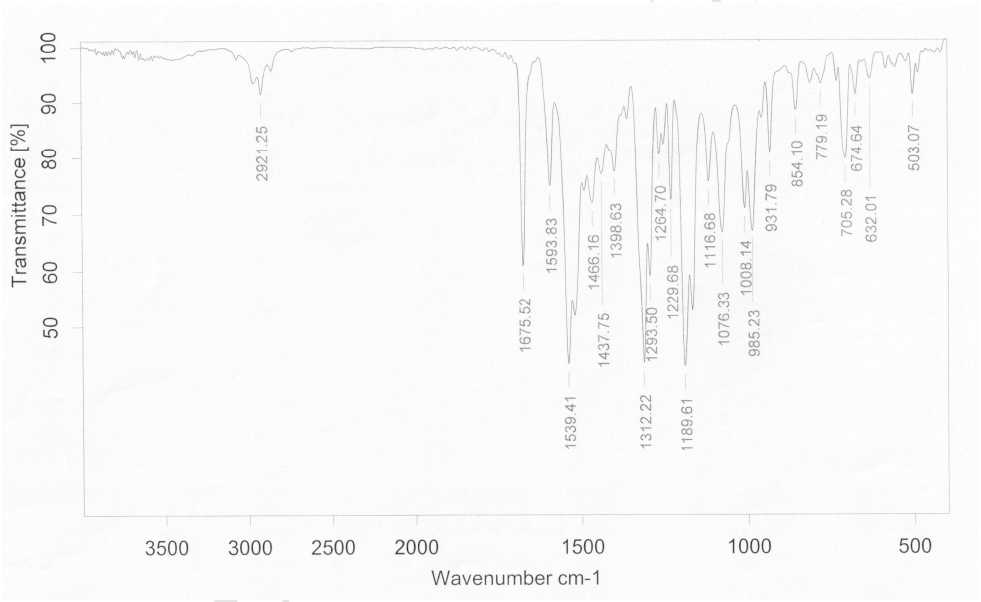

S2. Crystallographic data for compound 1

Table S2. Crystallographic data for compound 1

	1	**7**
Empirical formula	$C_{22}H_{25}BF_2N_2$	$C_{36}H_{31}BF_2N_2O_2$
Fw	366.25	572.44
temp (K)	173(2)	100(2)
Crystal description/color	block/orange	block/orange
Crystal system	orthorhombic	monoclinic
space group	P 2(1) 2(1)2(1)	P2(1)/n
a (Å)	7.8224(6)	7.9990(16)
b (Å)	13.4461(9)	19.843(4)
c (Å)	19.2506(14)	18.209(4)
α(deg)	90	90

β(deg)	90	92.56(3)
γ(deg)	90	90
Vol (Å^3)	2024.8(3)	2887.4(10)
Z	4	4
ρcalcul (mg· m^{-3})	1.201	1.317
μ □(mm^{-1})	0.082	0.090
F(000)	776	1200
Crystal size(mm^3)	0.63×0.33×0.28	0.13×0.11×0.07
θ range (deg)	2.60 to 27.51	2.05 to 25.00
Reflections collected/unique	1473/4604 [R(int)=0.0380]	16310/5078 [R(int) = 0.0878]
Absorption correction	Semi-empirical from equivalents	Semi-empirical from equivalents
Data/restraints/parameters	4604/0/251	5078/0/395
GOF on F^2	1.099	1.194
Final R indices [I>2σ(I)]	R1=0.0421, wR2=0.1092	R1=0.1371, wR2=0.3024
R indices (all data)	R1=0.0431, wR2=0.1102	R1=0.1538, wR2=0.3132
Largest diff. peak and hole, e/Å^3	0.253 and -0.198	0.483 and -0.330

S3. Experimental and calculated bond lengths and angles of compound 1

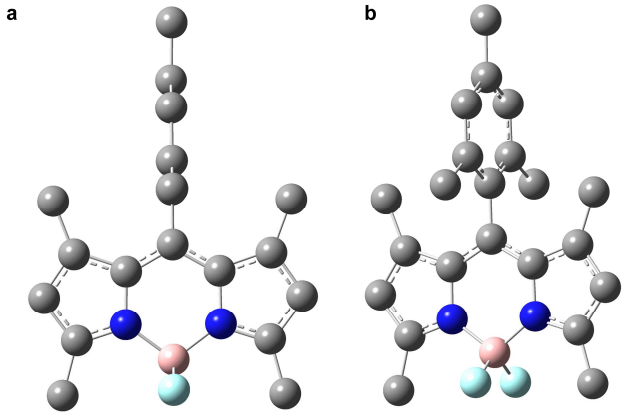

Figure S3. Calculated geometric structure of compound 1, a) front view, b) side view.

Table S3. Experimental and calculated bond lengths and angles of compound 1

Bonds and angles	X-ray	DFT-cal
B－N(average)(Å)	1.544	1.558
B－F(average)(Å)	1.392	1.394
C4－N1(Å)	1.348	1.347
C10－N2(Å)	1.355	1.347
C1－N1(Å)	1.396	1.400
C7－N2(Å)	1.395	1.400
C3－C4(Å)	1.404	1.410
C9－C10(Å)	1.402	1.410
N-B-N(deg)	107.22	106.13
F-B-N(average)(deg)	110.10	110.05

F-B-F(deg)	109.18	110.44

S4. Images demonstrating the colour **and visual fluorescence color of compounds 3-6**

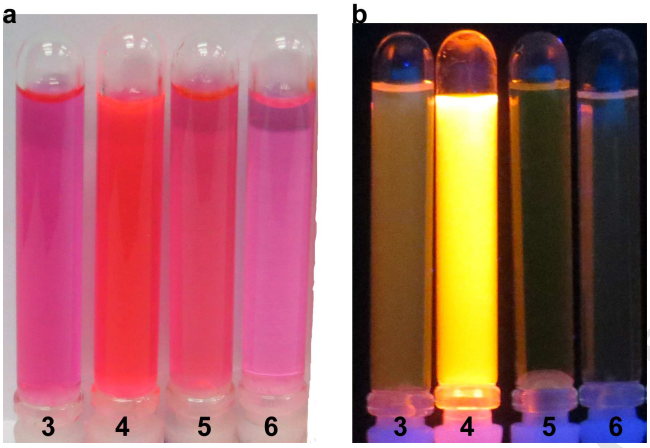

Figure S4. Images demonstrating the colour **(a) and visual fluorescence color (b) of compounds 3-6. The visual fluorescence color was obtained with excitation at 365 nm using a hand-held UV lamp.**

S5. The absorption and fluorescence spectra of compound 4 in different solvents and compounds 3-6 in CH_2Cl_2

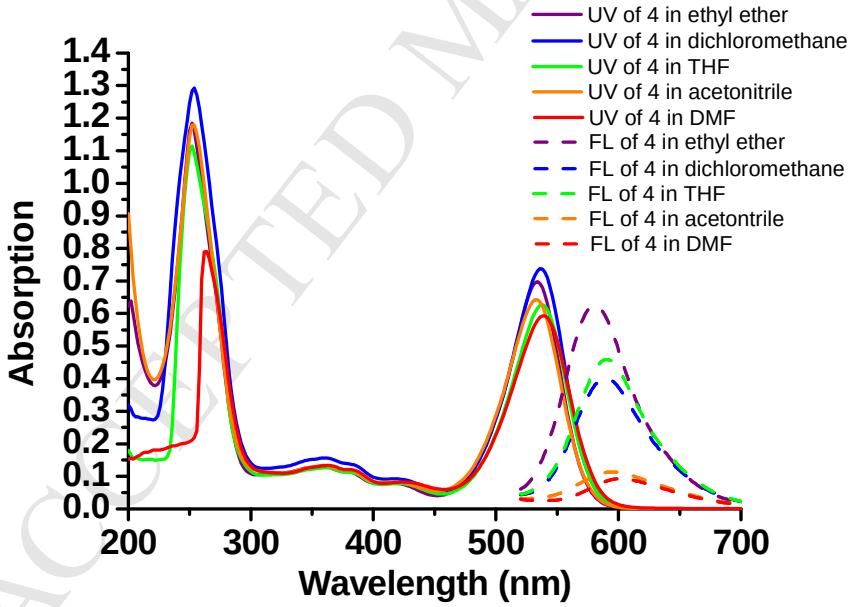

Figure S5-1. The absorption and fluorescence spectra of compound 4 in ethyl ether, dichloromethane, THF, acetonitrile and DMF

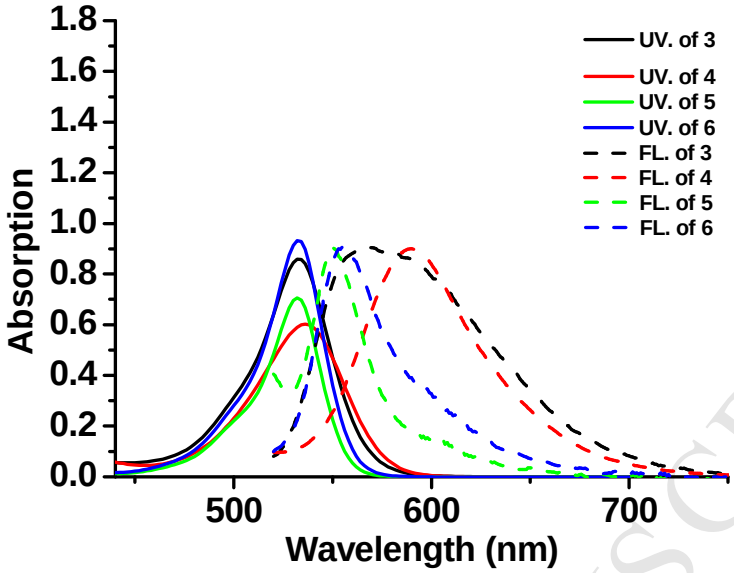

Figure S5-2. The absorption and fluorescence spectra of compounds 3-6 in CH_2Cl_2

S6. Calculated molecular orbital diagrams and energy levels of compounds 3-6

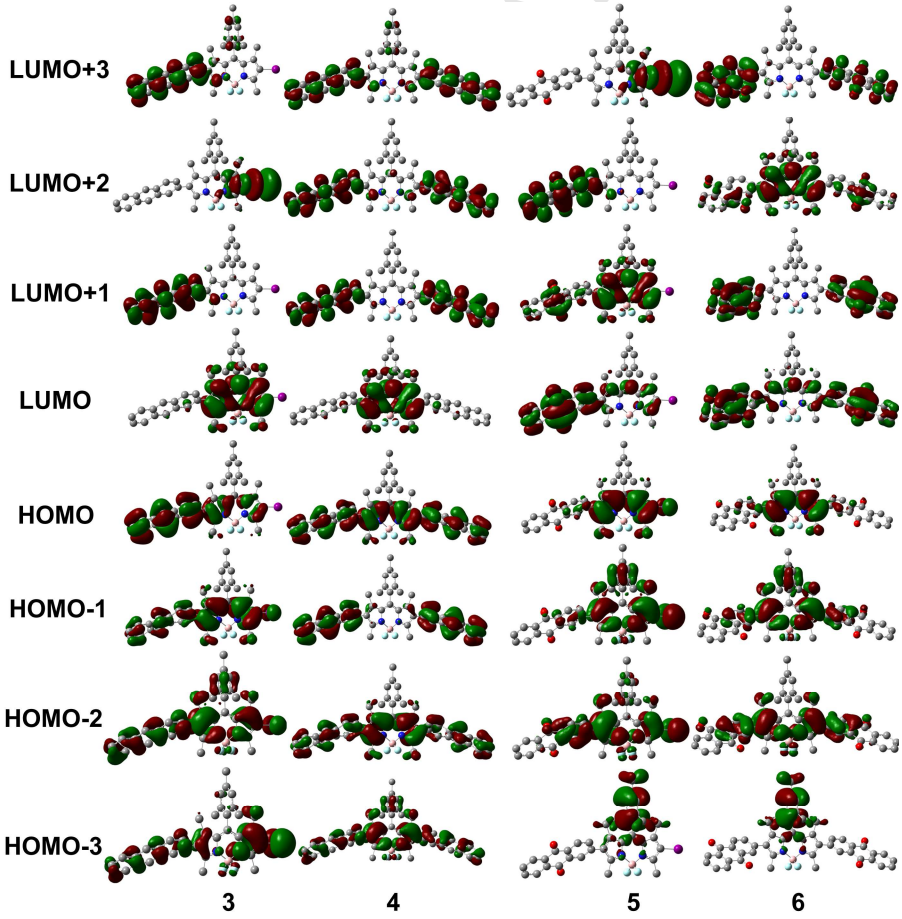

Figure S6. Calculated molecular orbital diagrams of compounds 3-6

Table S6. Calculated molecular orbital energy levels of compounds 3-6

Compound	**3**	**4**	**5**	**6**
LUMO+3(eV)	-0.47	-0.41	-0.73	-1.58
LUMO+2(eV)	-0.63	-1.68	-1.59	-2.63
LUMO+1(eV)	-1.75	-1.70	-2.67	-2.79
LUMO+0(eV)	-2.56	-2.43	-2.83	-2.84
HOMO-0(eV)	-5.26	-5.13	-5.61	-5.59
HOMO-1(eV)	-5.52	-5.24	-6.46	-6.46
HOMO-2(eV)	-6.31	-5.44	-6.57	-6.60
HOMO-3(eV)	-6.39	-6.19	-6.70	-6.70

S7. Calculated absorption wavelengths and oscillator strength of compounds 3-6

Table S7-1. Absorption wavelengths and oscillator strength of compound 3 evaluated by the TD-DFT (B3LYP/6-31tG*) calculation

Excitation energies (eV)	Absorption[nm](oscillator strength)	Assignments (%)
2.33	531.4 (0.07)	HOMO→LUMO (91)
3.23	384.1 (0.16)	HOMO-2→LUMO (58)
5.10	242.9 (1.50)	HOMO→LUMO+3 (14)
		HOMO-6→LUMO+1 (13)

Table S7-2. Absorption wavelengths and oscillator strength of compound 4 evaluated by the TD-DFT (B3LYP/6-31tG*) calculation

Excitation energies (eV)	Absorption[nm](oscillator strength)	Assignments (%)
2.37	523.7 (0.22)	HOMO→LUMO (84)
3.25	381.6 (0.16)	HOMO-3→LUMO (74)
4.45	278.5 (0.14)	HOMO→LUMO+3 (49)
		HOMO-2→LUMO+3 (23)

Table S7-3. Absorption wavelengths and oscillator strength of compound 5 evaluated by the TD-DFT (B3LYP/6-31tG*) calculation

Excitation energies (eV)	Absorption[nm](oscillator strength)	Assignments (%)
2.43	510.7 (0.12)	HOMO→LUMO (90)
3.20	388.0 (0.08)	HOMO-1→LUMO (28)
		HOMO-1→LUMO+1 (25)
4.43	280.1 (0.16)	HOMO-1→LUMO+2 (37)
		HOMO-2→LUMO+2 (31)

Table S7-4. Absorption wavelengths and oscillator strength of compound 6 evaluated by the TD-DFT (B3LYP/6-31tG*) calculation

Excitation energies (eV)	Absorption[nm](oscillator strength)	Assignments (%)

2.39	517.7 (0.26)	HOMO→LUMO (90)
3.25	381.1 (0.14)	HOMO-1→LUMO+2 (46)
		HOMO-2→LUMO+1 (21)